MET O 11 TECHNICAL NOTE NO 74

A SCHEME FOR THE OBJECTIVE ANALYSIS OF GATE DATA

MET O 11 ANALYSIS GROUP

Met O 11 (Forecasting Research Branch)
Meteorological Office
London Road
BRACKNELL
Berkshire
UK

November 1976

A SCHEME FOR THE OBJECTIVE ANALYSIS OF GATE DATA

MET O 11 ANALYSIS GROUP

CONTENTS

1. Introduction

The Tropical Research Group in the Meteorological Office took the unique opportunity of the GATE experiment to use data for testing their numerical modelling of the tropical atmosphere by comparisons with the real atmosphere. They therefore needed an objective analysis scheme which was to be run on a quasi-operational basis with analyses being produced every 12 or 24 hours, less than a day after data time, with the 12 or 24-hour forecast providing the background field for the next analysis.

The requirement was for surface pressure, upper air temperatures and winds in σ -coordinates ($\sigma = p/p^*$, where p^* is the surface pressure), and humidities by layers of the σ -coordinates. The area to be covered extended from 35°N to 15°S and 77°W to 49°E (Figure 1). A latitude/longitude grid was used with a spacing of 2°.

Because of the northerly latitude reached by the analysis area, and perhaps influenced by the mid-latitude experience of the objective analysis group, it was decided that a certain amount of balancing between the wind and the mass fields was desirable. It seemed advantageous to do this at a stage where information concerning data density and the reliability of the analyses was still available so that adjustments to the two fields could take this into account. The adjustment scheme used, which was based on the Numerical Variational Analysis of Sasaki (1970), required the solution of the Balance Equation in reverse (mass field from wind field), and since our previous experience had not extended to solving this in σ -coordinates it was decided to do the basic analyses of mass and velocity in pressure coordinates, adjust the fields, and then interpolate in the vertical into the σ -coordinates. Analyses of the humidity fields were carried out on σ surfaces, however. The method used was that described by Atkins (1974) and will not be elaborated further here. The analyses of contour height and wind components were done at pressure levels 1000, 950 (height only) 850, 700, 500, 400, 300, 250, 200, 150, 100 and 70 mb. It was originally intended to include the 30 and 10 mb levels but the quality and quantity of the data were too poor and climatological values were used instead.

There were other reasons for including an adjustment step. The basic analyses of each variable were obtained by the interpolation of observations of that variable using the process of optimum interpolation. The interpolation at each point required the solution of a number of simultaneous linear equations equal to the number of observations used; therefore the number of observations used to interpolate at each point needed to be limited for economy reasons. This introduced roughnesses which needed to be removed from the analyses. Also, by using some diagnostic relationship between the wind and mass variables, the adjustment process allowed values of one variable to help the analysis of the other variable. This was important in data sparse areas. In particular there were often large numbers of satellite wind vectors available for areas where there were few reliable observations of contour height - for instance over central South America and the southwestern parts of the tropical Atlantic.

The analysis scheme was followed by an initialisation process, basically one of dynamical initialisation after Nitta (1969), and consisted of a forward time step, followed by a backward time step, followed by a linear combination of the latest values and the values at the end of the previous iteration. All variables* were allowed to be adjusted during the course of the initialisation. During phase I of the GATE experiment, initialisation was applied for the equivalent of a 24-hour time integration. This was reduced to 6 hours in phases II and III.

The cycle of analyses and forecasts can be summarised as follows:

a. Derive wind and height background fields from the previous forecast, which verifies at time T, by interpolation from σ - to p- surfaces, except for relative humidity which was for model σ - layers.

b. Extract data for time T.

* other than moisture

c. Adjust background fields in the light of the observational data, and mutually adjust the wind and height fields using a variational analysis technique to give a preliminary set of analyses. After study of data and analyses by a monitoring team, insert corrections and bogus data as required and repeat for wind and height fields to give final analyses.

d. Interpolate from wind and height fields on pressure surfaces to wind and temperature fields for σ - layers and surface pressure.

e. Reduce high frequency waves by mutual adjustment of wind and mass fields in dynamic initialisation step.

f. Use model to advance fields from time T to time T + 12 (or 24).

2. Data

The data used came from radiosondes from ship and land stations, satellite sounding reports (SIRS), upper winds from pilot balloons, radar, rawinsondes or LOCATE systems, aircraft reports, satellite cloud vector reports (ATS and GOES), and surface reports from ships and land stations.

The satellite wind data were used from the ATS 3 satellite during Phase II and, following code changes necessitated by replacement of these data by SMS satellite data, from 4 September onwards in Phase III. Broadcasts used were principally the Global Trunk Circuit and Cyprus and Nairobi; Dakar broadcast became unavailable before GATE because of a change in transmission frequencies, but was received during part of Phase II and Phase III.

The distribution of stations for which data were sought is illustrated in Figure 2, a, b and c. Although the operational analyses were usually run about 24 hours after observation time, a large number of the observations which might have been available were, in fact, not received, or were not extracted due to errors in coding and transmission. The amount of data extracted increased progressively as the experiment proceeded, however; the number of reports extracted on this quasi operational scheme during phase III is shown in Table 1.

Analyses were done at fixed times and no attempt was made to adjust off-time observations in any way at all except to reduce their weight (increase their error variance) as their time discrepancy increased.

Winds from aircraft reports were used at the two nearest analysis levels, one above and one below, and were adjusted to take into account the vertical wind shear. The shears used were the forecast values available from the background fields. High-level and low-level ATS winds were allocated to the 250 mb and 850 mb levels respectively.

Where possible, radiosonde reports were corrected for systematic bias at all levels (Hawson and Caton (1961)). The 1000 mb analysis was done first to provide a reference level for the SIRS observations. The next level to be analysed was 70 mb and after this had been done, all radiosonde reports at this level were compared with the analysed fields and the differences, ϵ_{70} found used to estimate the errors at other levels in the sounding. Fractional corrections, ϵ_p were then made to the observed values at other pressure levels, p, such that

$$\epsilon_p = \epsilon_{70} \frac{\log \frac{p}{1000}}{\log \frac{70}{1000}}$$

Note that the radiosonde was rejected for $|\epsilon_{70}| > 300$ m. This procedure was repeated following the succeeding 100 mb analysis for radiosondes which only attained this level. Corrections for excessive warmth were also made to SIRS data,

as from 12Z 15 July. Corrections varied from 20 m at 850 mb to 40 m at 500 mb and 110 m at 70 mb.

3. The Background Field

Background fields for the optimum interpolation were obtained from the forecast model for both winds and heights. The forecast fields on sigma surfaces were first smoothed by means of a 17 point filter before interpolation to pressure levels. At 1000 mb, 950 mb and some parts of the 850 mb levels it was necessary for some downward extrapolation from the model forecasts to take place. At 70 mb the background field was a combination of 85% forecast and 15% climatology. Because the boundary values were kept unaltered in the forecasts, these were also basically persistence.

At the primary levels, i.e. 1000, 850, 500, 250, 100 and 70 mb, the background fields were used as they stood.* For the other (secondary) levels, i.e. 950, 700, 400, 300, 200 and 150 mb, they were modified both to give improved background fields and to help preserve the vertical consistency. The correction terms were formed by vertical interpolation of the difference between the analyses and background fields at the primary levels. Thus if δ_p is the difference between the analyses and background fields at any primary level, p, and d_p is the correction applied to the forecast field at a secondary level, d_p was taken as:

$$d_p = \frac{p - p_2}{p_1 - p_2} \delta p_1 + \frac{p_1 - p}{p_1 - p_2} \delta p_2$$

where p_1 and p_2 are two successive primary levels and p is a secondary level between them.

4. Error Assessments for Optimum Interpolation

Considerable effort went into the assessment of the variance of the errors of the observations, and of the background field. These influence the weights allocated to each observation during the optimum interpolation process. Values used were assessed from the literature and are summarised in Appendix 4. Note that different error values were used for corrected as against uncorrected radiosondes. It is important to note that the error variances required by the optimum interpolation process are not just the instrumental errors but should include the effects of scales of motion too small to be represented in the grid used. This is termed 'noise' and the optimum interpolation scheme assumes that it has no spatial correlations, though for a fuller discussion the reader is referred to Appendix 3.

For each wind component a noise value of 2.25 m^2 sec^{-2} was added to the estimated instrumental error variances. For contour height the values added varied with pressure level:

1000	950	850	700	500	400	300	250	200	150	100	70 mb
1.4	1.2	.75	1.5	2.4	3.4	4.2	5.1	6.1	6.1	6.1	6.1 m^2

The height values were first derived by taking estimated variances of observational error plus small scale prediction error (after Rutherford (1972)) and subtracting typical observational error variances appropriate to USA radiosondes. Such a procedure gave noise variances two orders of magnitude larger than the values quoted above. The reduction was made because in dealing with radiosonde heights the observational error variances ascribed (see Appendix 4) have already included in them some of the effects of noise - the observational error variances ascribed to each station being based on departures of the observed value from an analysed state, the latter having sub grid scale features removed. These values were found through experimentation to give reasonable results.

The assessment of errors of the background field, $\overline{\Delta^2}$, was problematical because no forecasts had been run on real data. An assessment of these was originally obtained prior to the start of the experiment from the climatological variability through the formula

* Apart from a double application of a 1-2-1 smoothing with effect from 14 September.

$$\Delta^2 = 2K^2\sigma_c^2(1-R(\Delta t))$$

a derivation of which is given in Appendix 1 together with the values of appropriate constants; K^2 is inversely proportional to the estimated skill of the model at any particular level and $R(\Delta t)$ is the autocorrelation of a meteorological variable over time interval Δt (12 or 24 hours). This expression gave error variances varying between 5 m^2 and 48 m^2 for heights and 2 m^2 sec^{-2} and 36 m^2 sec^{-2} for winds, depending on latitude and level. In running the scheme it became evident, however, that the estimates of error variance so obtained were far too optimistic and values over the chart were raised everywhere by 600 m^2 for heights and 9 m^2 sec^{-2} for winds at all levels. Later, during Phase II of the GATE experiment, a further large addition to the variances of the background fields was found to be necessary over the eastern part of the analysis region. There, background variances were raised a further 600 m^2 for heights and 36 m^2 sec^{-2} for winds with a linear adjustment into the rest of the background field between longitudes 18°E and 28°E. Thus, during the latter half of Phase II and in Phase III of the GATE experiment, the background field variances typically had the appearance of Figure 9a for heights and 9b for winds. This latter adjustment was found necessary because the background fields over the east African area were particularly poor, since this was a strong inflow region on many occasions (cf Figure 7a) with often little available data.

5. Data Checking

All the data had undergone quality control checks, but a further check was introduced before data was used in an analysis. The interpolated value was obtained at the observation point using the background field and observations other than the one in question. The observation of a variable s was rejected if it did not satisfy the criterion

$$|s_{observed} - s_{interpolated}| < c\sqrt{\overline{\epsilon_o^2} + \overline{E^2}}$$

where $\overline{\epsilon_o^2}$ is the variance of the observational error and $\overline{E^2}$ is the variance of the error of analysis (see below, §6). The criterion is based on the theory of maximum likelihood (Appendix 2). The constant c, can obviously be varied according to the severity of the test required; during GATE it was given values of $c = 6$ for heights, $c = 12$ for winds. Note that an observation with a large deviation is more likely to be accepted where the analysis is regarded as being unreliable and if the observation itself comes from an unreliable observation system. However in the latter case the weight that the observation is allotted in the analysis scheme will be small on this account.

In performing the data checking, two sweeps were made through the observations. At the end of the first sweep (made using only those data that had not been queried by the preceding data extraction quality control checks), a second sweep was made through those observations rejected by the first sweep and the observations reaccepted by the analysis if they now passed the check. This was in case observations were rejected in the first check by the inclusion of incorrect observations, not yet tested by the procedure, when making the estimates of the observation points in question. Those observations which remained were finally rejected as being incorrect.

In spite of these checks a considerable amount of human monitoring was required, correcting erroneous reports or inserting artificial ones where this was thought desirable. Considerable difficulty was encountered over the mountainous regions of East Africa, over South America and the South Western part of the tropical Atlantic and around the boundaries. In general, analyses were not amended subjectively unless they contained features that were obviously unrealistic.

6. Analysis Technique

The analysis of relative humidity was obtained using the scheme described by Atkins (1974). It is based on Cressman's successive approximation. It uses a weighting function which depends primarily on the distance of the observation from the grid point but is anisotropic in that it also depends on the gradient of the background field i.e. on the 12 or 24 hour forecast. The weighting

function falls off more rapidly in directions across the contour lines of the background field than for directions along the contour lines. This helps to preserve the shapes existing in the background fields and was found to be very advantageous in mid-latitudes.

The analysis process for the contour heights and winds was in two stages: first a horizontal interpolation to obtain values of contour height and wind independently at each grid point, which will be dealt with in this section, and secondly an adjustment stage, described in the next section, which allows the two fields to influence each other.

6.1 The Interpolation Scheme

For the first stage, Optimum Interpolation was used. This was based on the work of Gandin (1963), but using a forecast as a background field as described, inter alia, by Kruger (1969). It was decided to use optimum interpolation because the density of data varied considerably from one part of the area to another, and optimum interpolation can better cope with a spatially biased set of data than most other methods. In order to specify the scheme employed let us denote any one of the variables to be analysed by s; then we wish to form estimates $\bar{s}$ of the true values $\hat{s}_g$ of s at a set of grid points. So that we may form such an estimate at a grid point let us select a set of n observations, s_i, of s in the neighbourhood of the grid point where we also have a background value, $\tilde{s}_g$. If we can assume that we may also derive the background values at the observation points, then we can define a set of (n + 1) individual estimates of s at the grid point to be:

$$s_{iE} = s_i - \tilde{s}_i + \tilde{s}_g \qquad i = 1, n$$

$$s_{iE} = \tilde{s}_g = \hat{s}_g - \hat{s}_g + \tilde{s}_g \qquad i = n+1$$

and take our estimate of s to be given by a weighted mean of the individual estimates i.e. by

$$\bar{s} = \sum_{i=1}^{n+1} p_i s_{iE} \qquad \text{——— (1a)}$$

where we specify the constraint on the weights p_i that

$$\sum_{i=1}^{n+1} p_i = 1 \qquad \text{——— (1b)}$$

We now define the optimal set of p_i's as that set which minimises the mean square error of the analysis at the grid point, given the same configuration of observing stations on all occasions; i.e. defining $\overline{E^2} = \overline{(\bar{s} - \hat{s}_g)^2}$ where the bar represents a mean over many meteorological situations, we determine the optimal set of p_i's by solving the (n + 2) equations.

$$\left.\begin{aligned} \frac{\partial \overline{E^2}}{\partial p_j} &= \lambda \qquad j = 1, n+1 \\ \sum_{j=1}^{n+1} p_j &= 1 \end{aligned}\right\} \qquad \text{——— (2)}$$

where λ is the Lagrange undetermined multiplier of $\sum_{j=1}^{n+1} p_j = 1$
Substituting in $\overline{E^2}$ from (1) for $\overline{s}$ we obtain the set of equations

$$\frac{\partial}{\partial p_j}\overline{\left(\sum_{i=1}^{n+1} p_i s_{iE} - \hat{s}_g\right)^2} = \lambda \qquad j = 1, n+1$$

which yields the further set

$$2\overline{s_{jE}\left(\sum_{i=1}^{n+1} p_i s_{iE} - \hat{s}_g\right)} = \lambda \qquad j = 1, n+1$$

If we now write $s_{iE} = \hat{s}_g + \epsilon_i$, this gives us

$$2\overline{(\hat{s}_g + \epsilon_j)\left(\sum_{i=1}^{n+1} p_i \hat{s}_g - \hat{s}_g + \sum_{i=1}^{n+1} p_i \epsilon_i\right)} = \lambda \qquad j = 1, n+1$$

and using the condition $\sum_{i=1}^{n+1} p_i = 1$ we obtain

$$2\overline{(\hat{s}_g + \epsilon_j)\sum_{i=1}^{n+1} p_i \epsilon_i} = \lambda$$

Writing $\overline{\epsilon_i \epsilon_j}$ as a matrix $\{A_{ij}\} \equiv \underline{\underline{A}}$ and $\overline{\hat{s}_g \epsilon_i}$ as a vector $\{B_i\} \equiv \underline{B}$ we have the following equations for the weights, $\underline{p}$

$$\underline{\underline{A}} \cdot \underline{p} + (\underline{B} \cdot \underline{p})\underline{T} = \tfrac{1}{2}\lambda \underline{T} \qquad \text{(3a)}$$

$$\underline{T}^T \cdot \underline{p} = 1 = \underline{p}^T \cdot \underline{T} \qquad \text{(3b)}$$

($\underline{T}^T$: transpose)

where $\underline{T}$ is the vector such that $T_j = 1$ for $j = 1, n+1$.

From (3a) we deduce that

$$\underline{p} = \underline{\underline{A}}^{-1} \cdot \underline{T}\left\{\tfrac{1}{2}\lambda - \underline{B} \cdot \underline{p}\right\}$$

Using (3b) we have

$$\underline{T}^T \cdot \underline{p} = 1 = \underline{T}^T \cdot \underline{\underline{A}}^{-1} \cdot \underline{T}\left\{\tfrac{1}{2}\lambda - \underline{B} \cdot \underline{p}\right\}$$

Hence

$$\left\{\tfrac{1}{2}\lambda - \underline{B} \cdot \underline{p}\right\} = (\underline{T}^T \cdot \underline{\underline{A}}^{-1} \cdot \underline{T})^{-1}$$

and

$$\underline{p} = \underline{\underline{A}}^{-1} \cdot \underline{1} \Big/ (1^T \cdot \underline{\underline{A}}^{-1} \cdot 1) \qquad \text{——————} (4)$$

Thus we have obtained an expression for $\underline{p}$ in terms of the covariance matrix $\overline{\epsilon_i \epsilon_j}$. Now, since $s_{iE} = \hat{s}_g + \epsilon_i$ we have

$$\epsilon_i = s_{iE} - \hat{s}_g = s_i - \tilde{s}_i + \tilde{s}_g - \hat{s}_g \qquad i = 1, n$$

$$\epsilon_{n+1} = s_{iE} - \hat{s}_g = \tilde{s}_g - \hat{s}_g \qquad i = n+1$$

Let us now write $s_i = \hat{s}_i + \epsilon_{oi}$ where $\hat{s}_i$ represents the true value at the observation point and ϵ_{oi} the corresponding observational error. Then

$$\epsilon_i = \hat{s}_i + \epsilon_{oi} - \tilde{s}_i + \tilde{s}_g - \hat{s}_g \qquad i = 1, n$$

$$\epsilon_{n+1} = \tilde{s}_g - \hat{s}_g$$

If we now define Δ_i as the difference between the truth and the background fields at the point i and Δ_g as the corresponding quantity at the grid point i.e.

$\Delta_i = \hat{s}_i - \tilde{s}_i$ and $\Delta_g = \hat{s}_g - \tilde{s}_g$ then

$$\epsilon_i = \epsilon_{oi} + \Delta_i - \Delta_g \qquad i = 1, n$$

$$\epsilon_{n+1} = -\Delta_g$$

and, since we may assume that the observational errors are random so that ϵ_{oi} and ϵ_{oj} are correlated with nothing but themselves, then the terms of the matrix $\underline{\underline{A}}$ become

$$A_{ij} = \overline{\epsilon_i \epsilon_j} = \overline{\Delta_i \Delta_j} + \overline{\Delta_g \Delta_g} - \overline{\Delta_i \Delta_g} - \overline{\Delta_j \Delta_g} \qquad i \neq j \; ; \; i, j \neq n+1$$

$$A_{ii} = \overline{\epsilon_i \epsilon_i} = \overline{\Delta_i \Delta_i} - 2\overline{\Delta_i \Delta_g} + \overline{\Delta_g \Delta_g} + \overline{\epsilon_{oi}^2} \qquad i \neq n+1$$

$$A_{i,n+1} = \overline{\epsilon_i \epsilon_{n+1}} = \overline{\Delta_g \Delta_g} - \overline{\Delta_i \Delta_g} \qquad i \neq n+1$$

$$A_{n+1} A_{n+1} = \overline{\epsilon_{n+1} \epsilon_{n+1}} = \overline{\Delta_g \Delta_g} \qquad \text{——————} (5)$$

The terms $\overline{\Delta_i \Delta_j}$ are covariances of the errors of the background field (variances, for suffices which are identical). Thus if we can specify these quantities together with the variances of the observational errors we may determine the elements of $\underline{\underline{A}}$ from (5) and then solve (4) for our optimal weights $\{p_i\}$. It should be noted that the scheme defined by equations (1) and (4) is, except in the particular choice of the background field, formally identical to that derived by Gandin (1963). Note further that the mean square error of the analysis is given by

$$\overline{E^2} = \overline{\left(\sum_{i=1}^{n+1} p_i \epsilon_i \right)^2} = \sum_{\substack{i=1 \\ j=1}}^{n+1} \overline{(p_i \epsilon_i p_j \epsilon_j)} = \underline{p}^T \cdot \underline{\underline{A}} \cdot \underline{p}$$

whilst, from (4)

$$\underline{\underline{A}} \cdot \underline{p} = \underline{T} \Big/ (\underline{T}^T \cdot \underline{\underline{A}}^{-1} \cdot \underline{T})$$

$$\therefore \underline{p}^T \cdot \underline{\underline{A}} \cdot \underline{p} = \underline{p}^T \cdot \underline{T} \Big/ (\underline{T}^T \cdot \underline{\underline{A}}^{-1} \cdot \underline{T}) = (\underline{T}^T \cdot \underline{\underline{A}}^{-1} \cdot \underline{T})^{-1}, \text{ using (3b)}$$

$$\text{i.e. } \overline{E^2} = (\underline{T}^T \cdot \underline{\underline{A}}^{-1} \cdot \underline{T})^{-1} \qquad \text{——— 16)}$$

6.2 Covariances of Model Errors

The calculation of the weights involves the inversion of a matrix whose terms depend on the spatial covariances ($\overline{\Delta_i \Delta_j}$ etc) of model error for the particular element being analysed (equations (4) and (5)). We write these quantities in the form:

$$\overline{\Delta_i \Delta_j} = \left\{ \overline{\Delta_i^2} \cdot \overline{\Delta_j^2} \right\}^{1/2} \mu_{ij}$$

where the variances of model errors $\overline{\Delta_i^2}$ etc are derived as discussed in §4 and μ_{ij} is the spatial correlation for the element between points i. and j. During GATE it was assumed that μ_{ij} depends only upon the horizontal distance, r, between i. and j. and a correlation function chosen of the form

$$R(r) = \frac{1 - \frac{r^2}{2\eta^2}}{\left(1 + \frac{r^2}{\eta^2}\right)^{5/2}}$$

It is based on an empirical curve published by Rutherford (1972) and its form ensures that the implied error spectrum is positive for all wavelengths. The correlation function was assumed to be homogeneous and isotropic. η is a parameter which defines the width of the function. It was chosen so that R(r) = 0 at a distance equivalent to 20° of latitude (approx 2200 km) (Figure 3); this gives a broader function than is really true for fields in the tropics, particularly for the wind field, and results in a smoothing of the analyses. This seemed desirable in view of our lack of experience at that time.

6.3 Selection of Observations and Derivation of the Weights

The number of observations used for estimating the value of the field at each grid point was kept to 8 (cf. Kruger, 1969; Alaka and Elvander, 1972). A number of experiments had shown that raising the number to 12 made very little difference to the interpolated values, and did not warrant the doubling of the work involved. On the grounds that we should wish our 8 observations to be distributed as evenly as possible around the grid point (to remove any unwanted bias that might otherwise occur) the search for data was made according to quadrant about the analysis point as follows: The nearest synoptic wind (i.e. radar/omega/

rawinsonde) or radiosonde height in each quadrant was accepted provided it lay within the limiting distance. The number was made up to two in each quadrant by accepting the observation i. of any type with the largest value of

$$\frac{\overline{\Delta_i \Delta_g}}{(\overline{\Delta_i^2} + \overline{\epsilon_{oi}^2})}$$

this being the weight which an observation would have in the absence of all others; this allowed a good quality observation to be selected even though it was somewhat further away from the grid point than another observation which was less reliable. The total number of observations was made up to 8 (if necessary) by finally selecting observations irrespective of quadrant using the same parameter. An upper limit of six was placed on the number of observations chosen without regard to quadrant.

To make up the observation list for each grid point a substantial amount of sorting was required. This work was reduced considerably by dividing the analysis area into squares whose sides were of length equal to the largest distance at which an observation is accepted for analysis at a grid point. For each of these squares ('blocks') a directory of available observations was made. Thus when assembling a list of observations for any grid point it was only necessary to examine the nine blocks centred on the block which contains the grid point. This resulted in a significant time saving.

The set of linear equations for the weights (equation (4)) were solved by the method of Choleski (e.g. Hartree, 1958, p.180). Such a set of equations can, however, become ill-conditioned when two observations used in the interpolation are much closer to each other than either is to the grid point in question, especially when all three points fall on a straight line. The result is an interpolated value that can often be quite erroneous. In the version of optimum interpolation used there was a constraint such that the sum of the weights of the observations was unity. It was found by experiment that the problem could be dealt with by testing for any observation weight which was less than -0.5, searching for the nearest observation to this one, and combining the two into one observation by taking their average and placing it at the average position. The weights were then re-calculated treating the combined observation as one observation. An essential assumption in the optimum interpolation method is that errors in observations are spatially uncorrelated. This is not true when observations are very close together because of the presence of sub-grid-scale waves (Appendix 3). One way of treating this problem is to throw away a large number of the observations, but this is wasteful, particularly where there is a large number of low quality observations; each observation can contribute some information to the analysis, but not very much. Cressman's successive approximation technique has the advantage of being able to use an unlimited number of observations but does not take their distribution into account. In the present scheme all surface observations which lay within a 1° square of latitude and longitude were averaged and the value allocated to their average latitude and longitude. This "super-ob" could be expected to have a smaller error variance than the original observations, although the original error value was actually used. Not only did this mean that we are making use of more observations but it also reduces the possibility of ill-conditioning.

7. Adjustment Stage

7.1 Theoretical background

Up to this stage the analyses of contour height and wind are independent of each other, apart from the fact that the background fields of both are derived from the dynamical equations of the prediction model. The adjustment used is based on the Numerical Variational Analysis due to Sasaki (1970), using a form of "weak constraint" in his "timewise localised" form; a form used successfully by Lewis and Grayson (1972). Carrying out this step helps to allow the field of one variable to adjust to features on another and to cut down the time necessary for initialisation.

In our case the variational integral to be minimised is taken to be

$$I = \iint \left[\alpha(\underset{\sim}{V}-\tilde{\underset{\sim}{V}})^2 + \beta(h-\tilde{h})^2 + \gamma \left\{ g\nabla(h-h_b) + f\,\underset{\sim}{k}\times(\underset{\sim}{V}-\tilde{\underset{\sim}{V}}) \right\}^2 \right] dS$$

where $\underset{\sim}{V}$ = final value of the velocity field

$\tilde{\underset{\sim}{V}}$ = initial (analysis) value of the velocity field

h = final value of the height field

$\tilde{h}$ = initial (analysis) value of the height field

h_b = height field obtained from $\tilde{\underset{\sim}{V}}$ by solving the balance equation.

$\underset{\sim}{k}$ = unit vertical vector,

the parameters α, β, and γ being predetermined. The first two terms are to keep the departures from the analysed fields to a minimum. Bearing in mind the fact that h_b and $\tilde{\underset{\sim}{V}}$ satisfy the balance equation, the third term requires that departures of $\underset{\sim}{V}$ and h from the balance equation should approximately be in geostrophic balance, the extent to which this constraint is satisfied depending on the size of γ relative to α and β. Note that near the equator the term $f\,\underset{\sim}{k}\times(\underset{\sim}{V}-\tilde{\underset{\sim}{V}})$ is negligible so that there $\underset{\sim}{V}$ will be very close to $\tilde{\underset{\sim}{V}}$ and the value of h close to $\tilde{h}$, but the shape (gradients) of h will be close to those of h_b.

Minimising I with respect to arbitrary variations of $\underset{\sim}{V}$ and h with use of the vector identity

$$\iint \underset{\sim}{F}\cdot\nabla(\delta a)\,dS = \iint \nabla\cdot(\underset{\sim}{F}\delta a)\,dS - \iint (\nabla\cdot\underset{\sim}{F})\,\delta a\,d\underset{\sim}{S}$$

($d\underset{\sim}{S}$: element of area.)

$$= \int (F\delta a)\cdot d\underset{\sim}{s} - \iint (\nabla\cdot\underset{\sim}{F})\,\delta a\,dS$$

($d\underset{\sim}{s}$: line element.)

and setting $\delta h = 0$ around the boundary, we obtain the equations

$$\alpha(\underset{\sim}{V}-\tilde{\underset{\sim}{V}}) + \gamma f\,\underset{\sim}{k}\times\left\{ g\nabla(h-h_b) + f\,\underset{\sim}{k}\times(\underset{\sim}{V}-\tilde{\underset{\sim}{V}}) \right\} = 0 \qquad \text{——(7)}$$

$$\beta(h-\tilde{h}) - \nabla\cdot\left[\gamma \left\{ g\nabla(h-h_b) + f\,\underset{\sim}{k}\times(\underset{\sim}{V}-\tilde{\underset{\sim}{V}}) \right\} \right] = 0 \qquad \text{——(8)}$$

Eliminating $\underset{\sim}{V} - \underset{\sim}{\tilde{V}}$ yields the elliptic equation

$$\nabla \cdot (r \nabla h) - \beta h = \nabla \cdot (r \nabla h_b) - \beta \tilde{h} \qquad \text{——— (9)}$$

which we are required to solve for h and where $r = \gamma g^2 \alpha / (\alpha + \gamma f^2)$

Rearranging (7) gives

$$V - \underset{\sim}{\tilde{V}} = \frac{\gamma g}{\alpha + \gamma f^2} f \underset{\sim}{k} \times \nabla (h - h_b)$$

or, in component form

$$\left.\begin{aligned} u - \tilde{u} &= - \frac{g \gamma f}{\alpha + \gamma f^2} \frac{\partial}{\partial y} (h - h_b) \\ v - \tilde{v} &= \frac{g \gamma f}{\alpha + \gamma f^2} \frac{\partial}{\partial x} (h - h_b) \end{aligned}\right\} \qquad \text{——— (10)}$$

7.2 Solution of the balance equation for h_b

Before equations (9) and (10) can be solved to give the final adjusted fields (h, u, v) it is necessary to derive the field h_b from $\underset{\sim}{\tilde{v}}$ through the balance equation. The form of the balance equation used in the present scheme may be derived by taking the two dimensional divergence of the equations of motion written in spherical polar coordinates, neglecting the vertical motion terms and setting

$$\frac{\partial D}{\partial t} \leftarrow \text{divergence} = \frac{\partial u}{\partial \lambda} + \frac{\partial}{\partial \phi} (v \cos \phi) = 0$$

Thus we have

$$\frac{1}{\cos^2 \phi} \frac{\partial^2 h}{\partial \lambda^2} + \frac{1}{\cos \phi} \frac{\partial}{\partial \phi} \left(\frac{\partial h}{\partial \phi} \cos \phi \right)$$

$$+ \frac{1}{g \cos \phi} \left[\frac{1}{\cos \phi} \frac{\partial}{\partial \lambda} \left(u \frac{\partial u}{\partial \lambda} \right) + \frac{\partial}{\partial \lambda} \left(v \frac{\partial u}{\partial \phi} \right) - \frac{\partial}{\partial \lambda} (uv \tan \phi) + \frac{1}{\cos \phi} \frac{\partial}{\partial \phi} \left(u \cos \phi \frac{\partial v}{\partial \lambda} \right) \right.$$

$$\left. + \frac{\partial}{\partial \phi} \left(v \cos \phi \frac{\partial v}{\partial \phi} \right) + \frac{\partial}{\partial \phi} (u^2 \sin \phi) + R \left\{ - \frac{\partial}{\partial \lambda} (fv) + \frac{\partial}{\partial \phi} (fu \cos \phi) \right\} \right]$$

$$- \frac{R}{\cos \phi} \left[\frac{\partial}{\partial \lambda} \left(\frac{\partial \gamma_{\lambda \phi}}{\partial p} \right) + \frac{\partial}{\partial \phi} \left(\cos \phi \frac{\partial \gamma_{\lambda \phi}}{\partial p} \right) \right] = 0 \qquad \text{——— (11)}$$

where, for clarity, we have written h for h_b and (u, v) for $(\tilde{u}, \tilde{v})$. R is the radius of the earth and ϕ and λ represent latitude and longitude respectively. We solve equation (11) numerically by ADI techniques (e.g. Wachspress; 1966).

The friction terms were parameterised in a similar fashion to the method of Lewis and Grayson (1972) by taking the stress at 1000 mb to be given by

$$\tilde{\tau}_{1000} = K \tilde{V}_{1000}$$

and assuming a linear variation of stress with the vertical pressure coordinate to a constant zero value at 900 mb and above. Thus friction was included for the 1000 mb and 950 mb levels only, where $\partial \tilde{\tau} / \partial p$ was taken to be

$$\frac{\partial \tilde{\tau}}{\partial p} = -\frac{K}{\Delta p} \tilde{V}_{1000}$$

with $\frac{K}{\Delta p}$ having values 1.2×10^{-6} and 2.4×10^{-6} over sea and land respectively.

7.3 The Variational Step

Once the field h_b had been derived the variational step could be carried out; equation (9) was solved numerically for the adjusted field h by successive over-relaxation (e.g. Haltiner, 1971, p.111), after which the adjusted wind components were readily derived through equation (10). The weights α and β were taken as being inversely proportional to the estimated variance of the error of the relevant analysis at each particular point. These could, of course be obtained from the optimum interpolation process (equation (6)). These parameters therefore varied over the grid. Thus where either of the analyses could be regarded as reliable, it would not be changed very much; where one of the analyses could be regarded as being unreliable it would tend to be altered to make the constraint more closely satisfied. γ was taken as a constant and a fairly small value was chosen so that the fields were not modified except where the error variances indicated that they were particularly unreliable. Strictly γ^{-1} represents the mean square value of

$$\left\{ g\nabla(h-h_b) + f\,\underset{\sim}{k} \times (\underset{\sim}{V} - \tilde{\underset{\sim}{V}}) \right\}$$

Note that equation (10) i.e.

$$\underset{\sim}{V} - \tilde{\underset{\sim}{V}} = \frac{\gamma g}{\alpha + \gamma f^2} f\,\underset{\sim}{k} \times \nabla(h-h_b)$$

implies that when f is small, $\underset{\sim}{V}$ is virtually independent of the corrections to the height field whilst if were chosen to be large, the relationship would reduce to a geostrophic relationship between $(\underset{\sim}{V} - \tilde{\underset{\sim}{V}})$ and $(h-h_b)$.

It should be further noted that the adjustment process was applied independently to each level.

8. Overall Scheme

Figure 4 shows the outline of the overall scheme. As noted earlier the first level to be analysed is 1000 mb - this is required to provide a reference level for the SIRS data.

Next follow the 70 mb and 100 mb analyses, each followed by radiosonde corrections. Analyses at 850, 500 and 250 mb are then made simultaneously and the results at these levels are used to adjust the background fields of heights and winds at all the remaining levels, thus ensuring a degree of vertical consistency this also reduces the number of levels at which bogus data needs to be inserted when the analyses require amending on a subjective basis.

One disadvantage of the scheme in practice was that data outside the area of analysis was not included in the analysis procedure. Since the forecast model holds boundary values constant, this omission led to excessive roughnesses and unrealistic features near the edges of the area during the early part of the experiment. This was controlled by introducing a smoothing of the background fields around the outermost rows of points.

9. Some Results

The remaining diagrams (Figures 5 to 8) show examples of the analyses computed during the GATE experiment.

Figure 5a illustrates grid point values of wind at 850 mb and shows several features of interest in the low level flow. Prominent among these are the easterly trade wind flow over the Atlantic; north to northwest winds over the Middle East and southerly cross-equatorial flow off East Africa. Particularly noticable is the series of vortices stretching across Africa north of the equator and out into the Atlantic. Satellite photographs taken on this day show a band of cloud at about 5-8°N extending across much of the Atlantic in the centre of a broad convergence zone, detectable from the wind pattern. Cloudy areas can also be associated with the vortices at about 14°N 122°W and 8°N, 5°W. For comparison Figure 5b shows a hand-drawn streamline analysis at 850 mb and is a copy of an analysis produced at Dakar during the GATE experiment.

Figure 6, a to c, shows more detailed comparisons of wind data, objective analyses and subjective analyses, the latter again being made in Dakar during the GATE period. The charts are drawn for 12Z, 2 September 1974 for 1000 mb. The objective and subjective analyses show good agreement on the broad scale, but details of the smaller-scale features such as convergence lines and centres differ. The subjective analyses are neater and more consistent in these areas than the objective analyses, but nevertheless the latter are reasonably consistent with the existing observations.

Figure 7, a and b, illustrates the wind and contour height analyses at 250 mb on yet another occasion, and Figure 7c is the hand-drawn streamline chart for 200 mb for the central GATE area. The height analysis shows slack gradients in equatorial latitudes, and there is good correlation between patterns of contour height and wind flow beyond about 15°N.

Some comparisons of velocity and contour height fields before and after the variational step (Figure 8, a to c) show that the two fields are modified in a sensible way. Since the solution of the reverse Balance Equation is very smooth in low latitudes the net effect was a smoothing of small scale features from the height field unless they corresponded to features in the wind field. The independently analysed fields of wind and contour height for a particular occasion are shown in Figure 8, a and b. In Figure 8c, the height field is shown after application of balance using the Sasaki variational step. It will be seen that height gradients are much reduced, especially over equatorial regions. The centre over Venezuela, which is not represented in the wind flow and has probably originated from an isolated erroneous report, is considerably damped in Figure 8c. Further away from the equator, smoothing is still present but the two fields appear to have interacted in a more positive way.

10. Summary and Comment

There is undoubtedly much room for improvement in this analysis scheme. In particular not enough attention is paid to the vertical structure and hence to the temperature and stability fields. Also it might be better if the analyses were done in σ coordinates as the interpolation to and from the pressure coordinate system gives rise to considerable roughnesses in the fields presented to the time integration particularly near mountainous regions.

More study of the structure functions involved would lead to improvements in the depiction of details in areas of dense data.

Analysis of meteorological charts in tropical regions is normally a highly subjective process. Most hand drawn analyses are limited to representation of flow patterns by streamlines and isotachs, and consistency in time is difficult to achieve. It has been difficult so far to make any direct assessments yet on the success of the GATE analyses, but investigations by the Tropical Research Group in the Meteorological Office show that in these analyses and forecasts there are trough lines which keep a reasonable progression and consistency over a period of several days, and this is very encouraging.

11. Acknowledgements

The analysis scheme was devised by scientists of the Forecasting Research Branch, primarily Mr D E Jones, Dr A Belyavin and Dr S Clough. Much of the practical work in implementing the procedure was carried out by Miss M K Hinds and Mr C S Clarke.

This Technical Note was drawn largely from papers and reports by Mr D E Jones, partly from an MRC paper by Mr P Graystone and was collated by Dr H Cattle.

References

Alaker M A and Elvander R C	1972	Optimum interpolation from observations of mixed quality. Mon.Weath.Rev. 100, 8, p.612.
Atkins M J	1974	The Objective Analysis of Relative Humidity. Tellus 26, 6, p.663
Gandin L S	1963	Objective Analysis of the Meteorological Fields. Gidrometeoizdat. Translated by the Israel Program for Scientific Translations Jerusalem, 1965.
Haltiner G J	1971	Numerical Weather Prediction. Wiley.
Hartree D R	1958	Numerical Analysis, Clarendon Press, Oxford. Second Edition.
Hawson, C L and Caton P G F	1961	A synoptic method for the international comparison of geopotential observations Met Mag 90, 12, p.336.
Kruger H B	1969	General and Special Approaches to the Problems of Objective Analysis of Meteorological Variables. Quart.J.R.Met.Soc 91 p. 87.
Lewis J M and Grayson T H	1972	The Adjustment of Surface Wind and Pressure by Sasaki's Variational Matching Technique. J.Appl.Met.11 4 p.586.
Nitta T	1969	Initialisation and Analysis for the Primitive Equation Model. Proceedings of the WMO/IUGG Symposium on Numerical Weather Prediction, Tokyo. Nov 26-Dec 4 1968, Japan Meteorological Agency, Tokyo.
Rutherford I D	1972	Date Assimilation by Statistical Interpolation of Forecast Error Fields. J Atmos Sci.29. p.809.
Sasaki Y	1970	Some Basic Formalisms in Numerical Variational Analysis - Monthly Weath. Review 98; 12.
Tucker G B	1960	Upper Winds over the World. Part III. Geophysical Memoirs No 105. MO London HMSO.
Wachspress E L	1966	Iterative Solution of Eliptic Systems and Applications to the Neutron Diffusion Equations of Reactor Physics. International Series in Applied Mathematics, Prentice Hall.

TABLE 1

Reports extracted daily during Phase 3 (29 August - 19 September 1974)

		Average	Max	Min
Upper Air temp)	Land	71	81	61
Upper Air wind)		97	120	66
Upper air ship		24	33	13
Surface land		532	619	398
Surface ships		168	200	114
Aircraft reports		63	90	47
SIRS		60	82	21
Satellite Winds		280*	408	118

*4-19 September

Statistics relate to observations made at 1200 GMT or centred on 1200 GMT for satellite and aircraft reports.

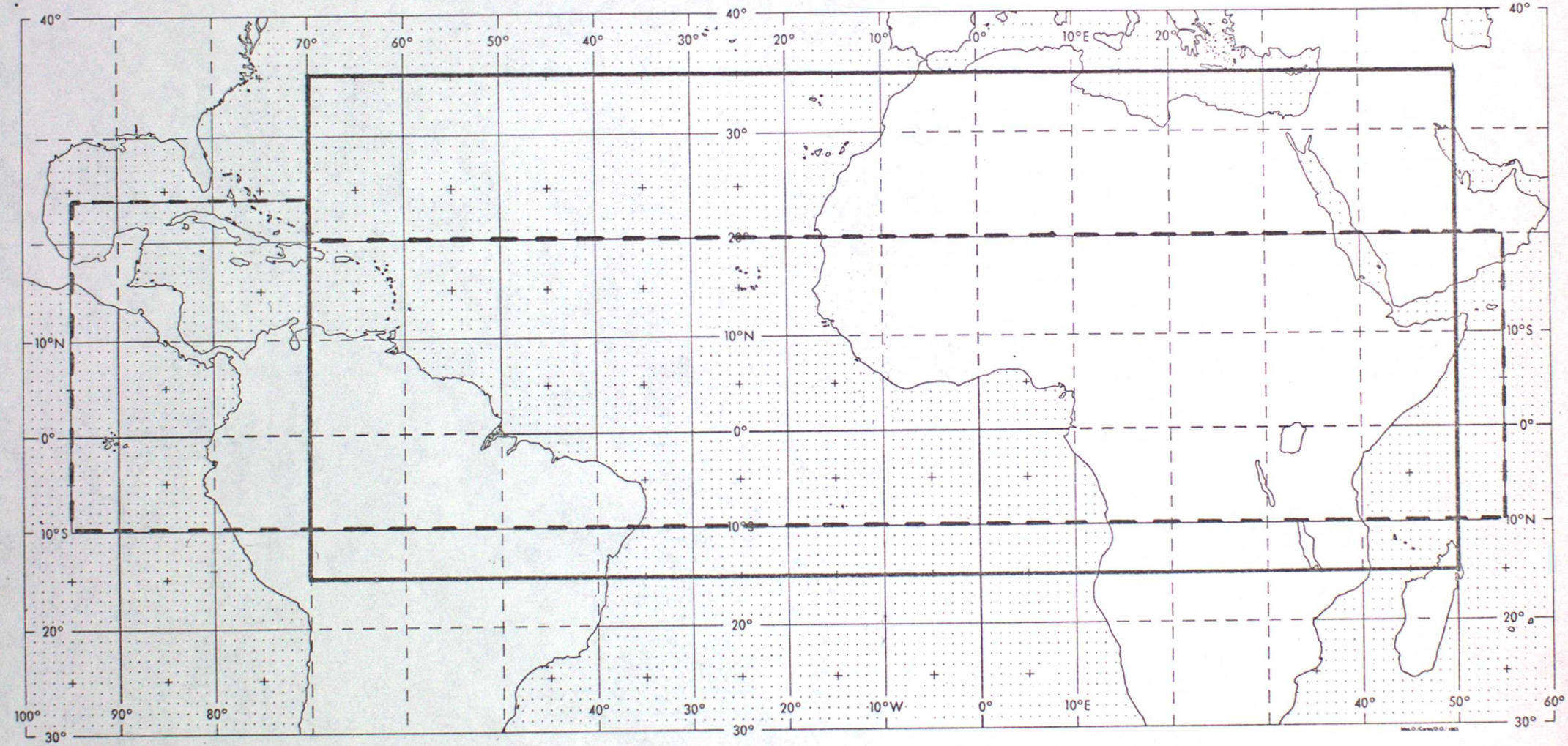

Figure 1 The area enclosed by the heavy pecked line is the GATE 'A scale' area. The heavy solid line encloses the area of analysis for the present scheme.

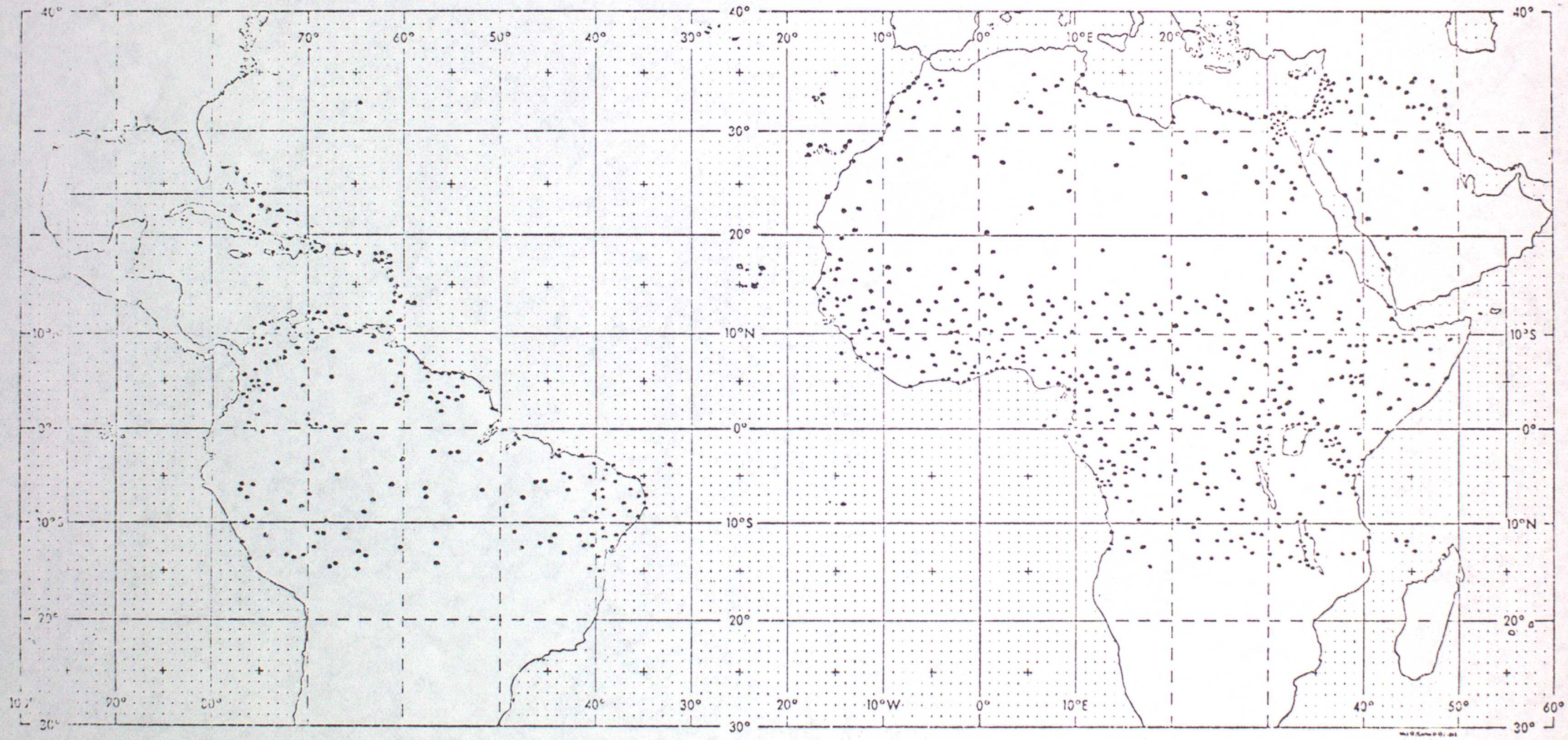

Figure 2a Land surface observing stations.

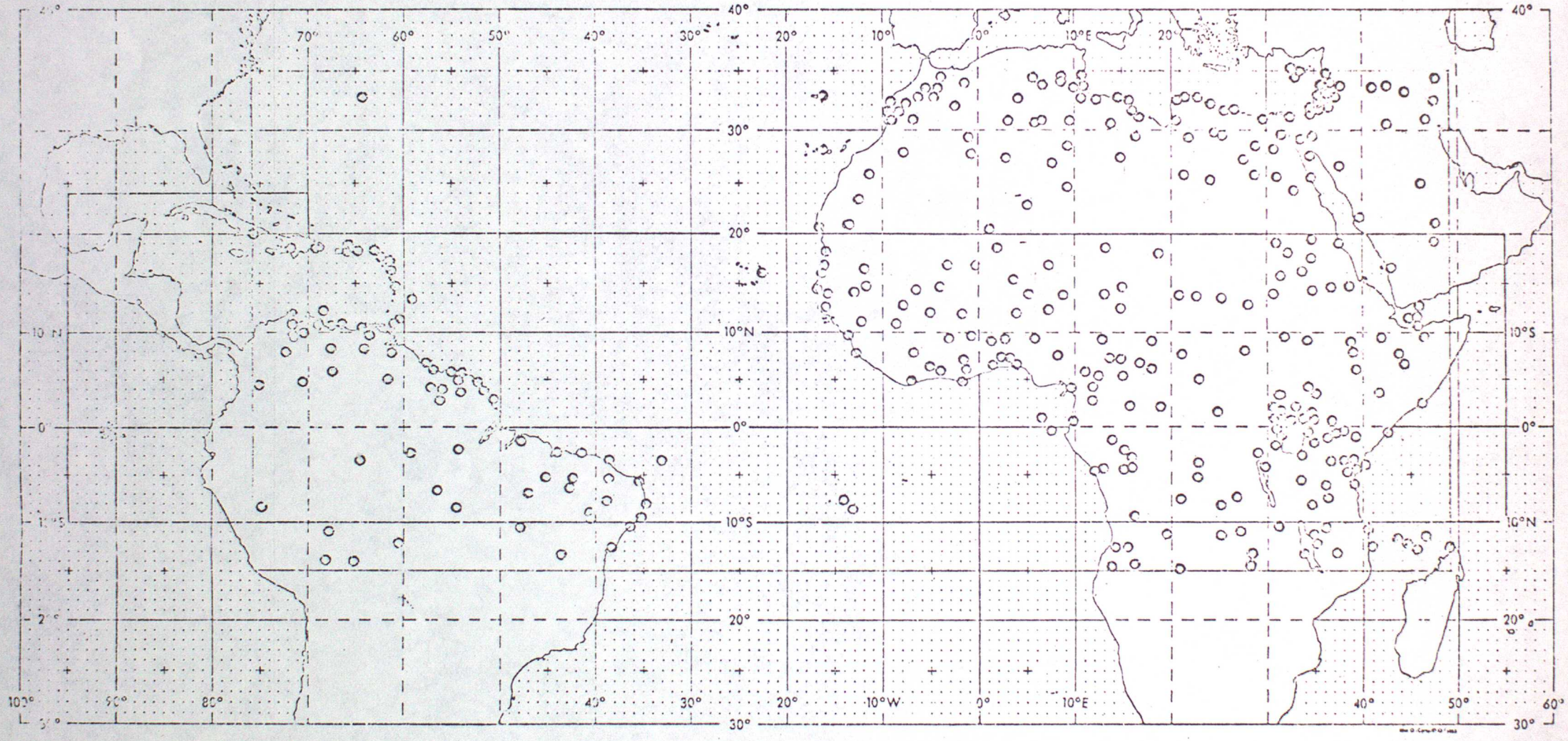

Figure 2b. Upper air observing land stations.

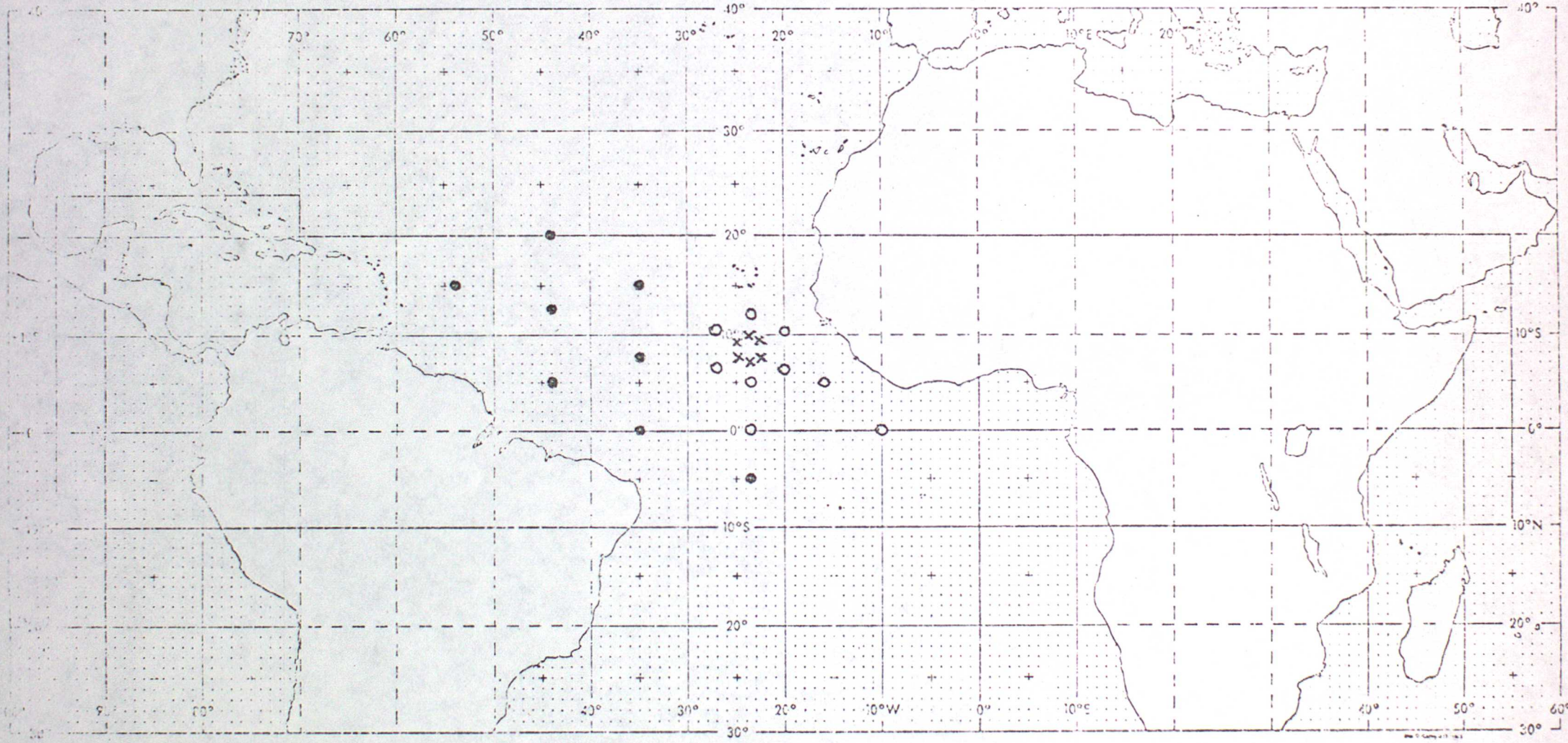

Figure 2c A and B-scale ship distribution (Phase I) × A-scale; ○ A/B scale; ● B-scale.

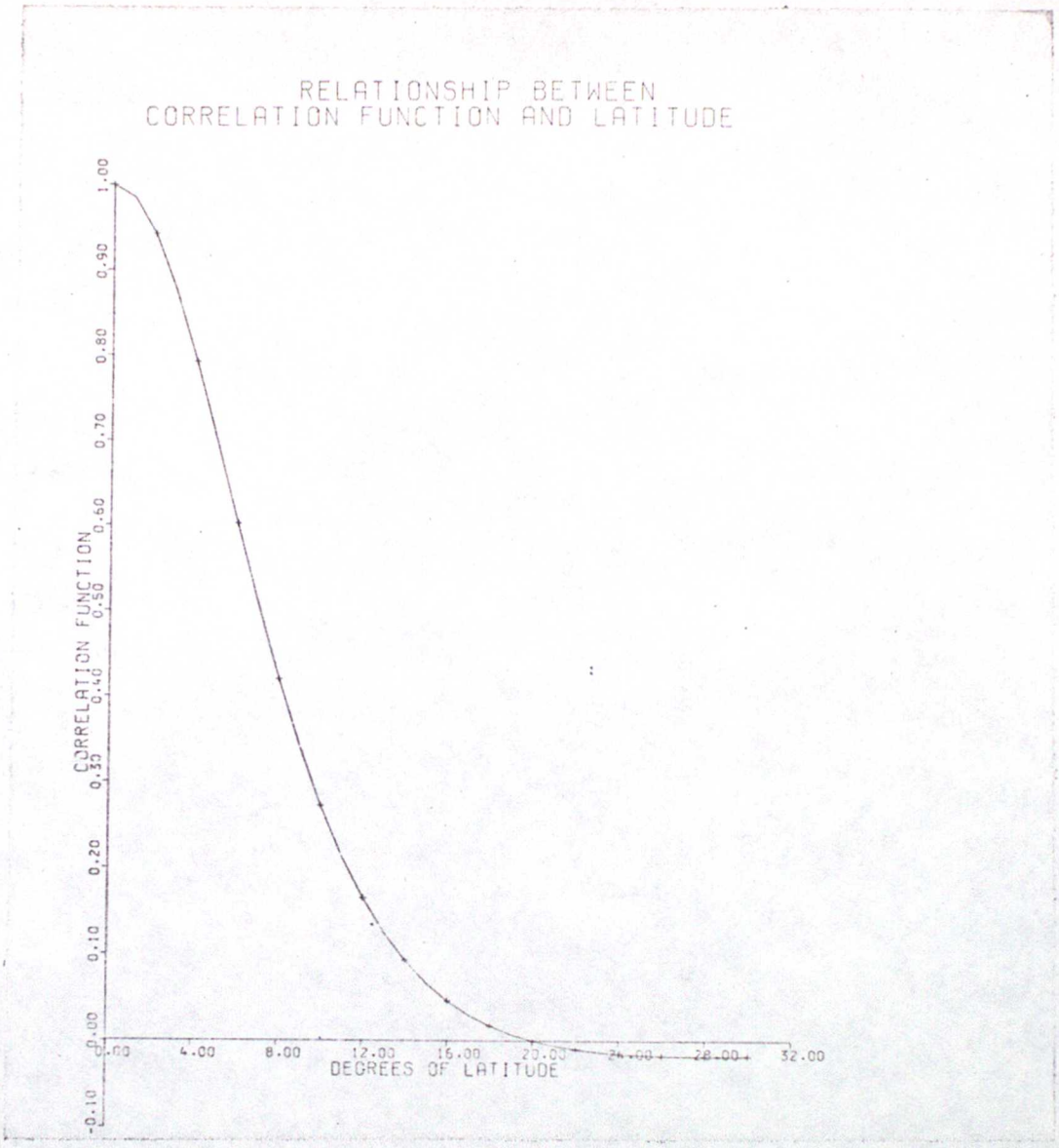

Figure 3 Correlation function for model errors used during GATE,

$$\mu(r) = \left(1 - \frac{r^2}{2\eta^2}\right) \Big/ \left(1 + \frac{r^2}{\eta^2}\right)^{5/2} ; \quad \eta = 0.005 \text{ with r}$$

in degrees of latitude.

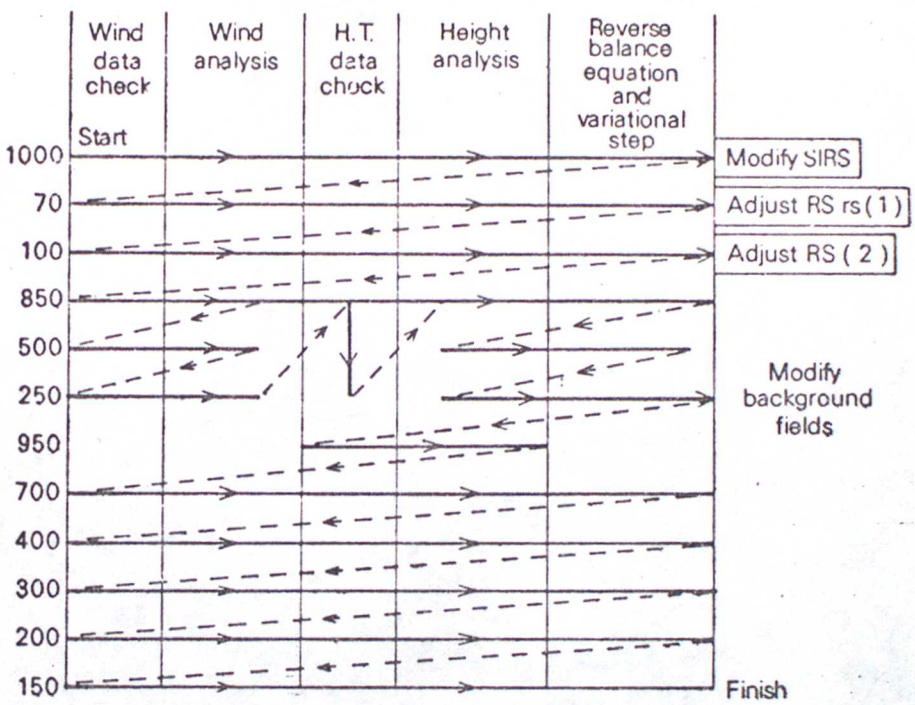

Figure 4 Outline of GATE analysis scheme.

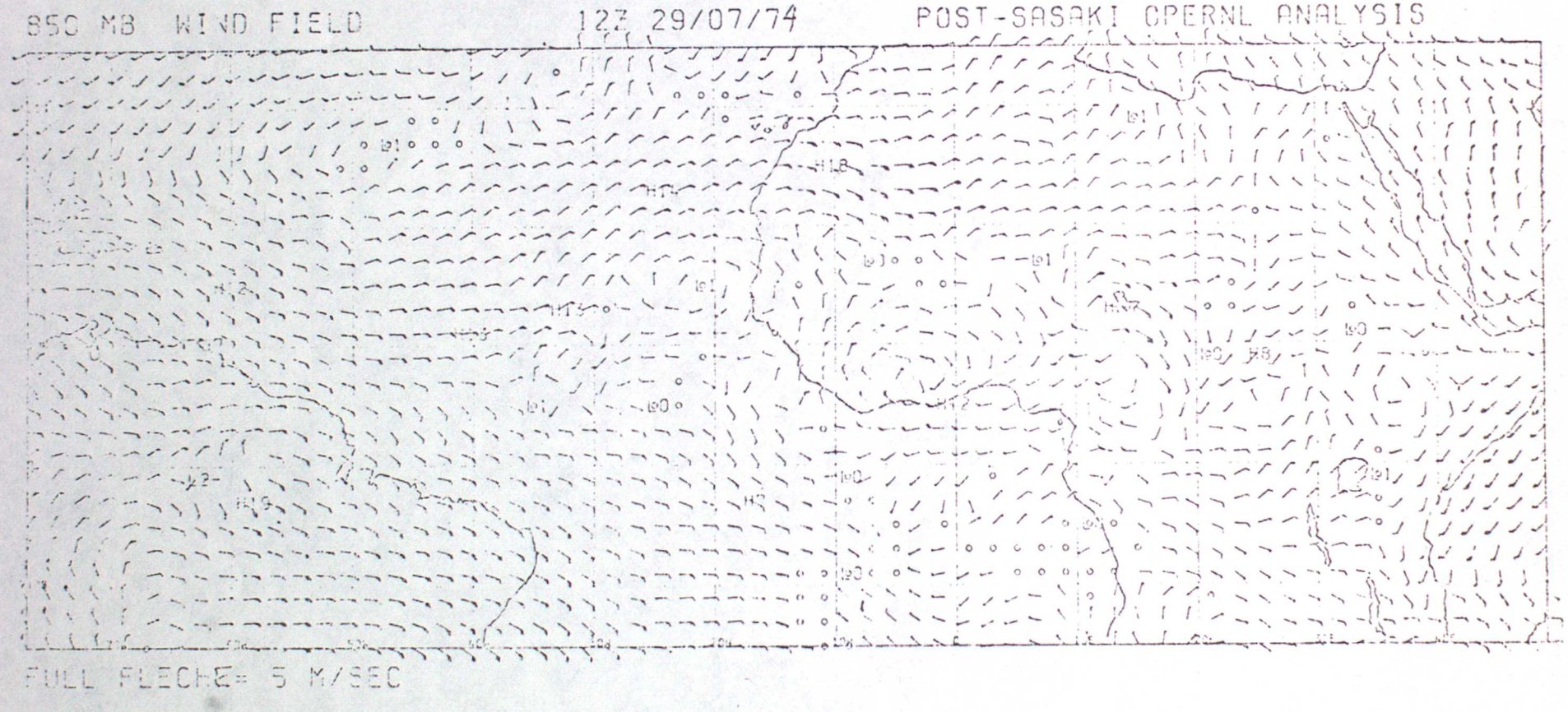

Figure 5a Objective analysis of winds at 850 mb for 12Z 29 July 1974.

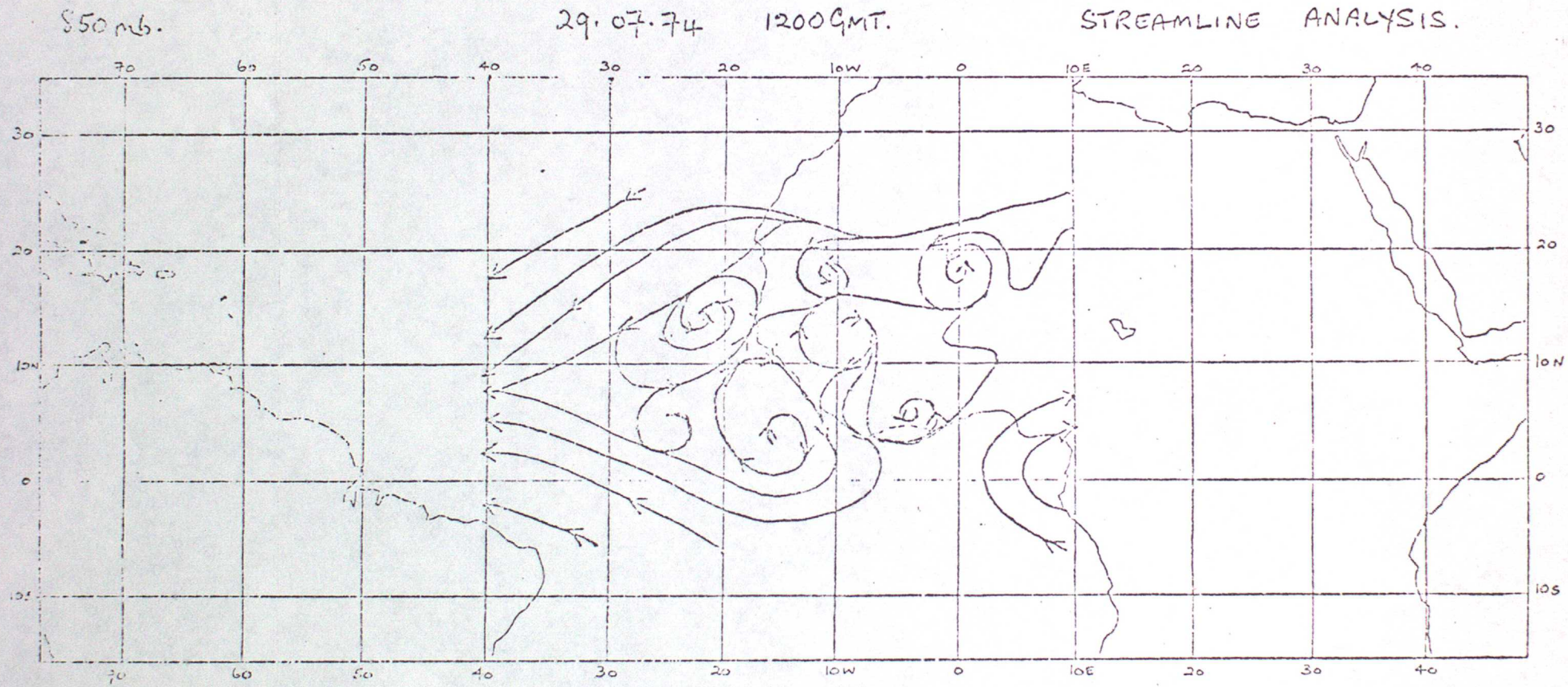

Figure 5b Hand-drawn 850 mb streamline analysis for 12Z 29 July 1974.

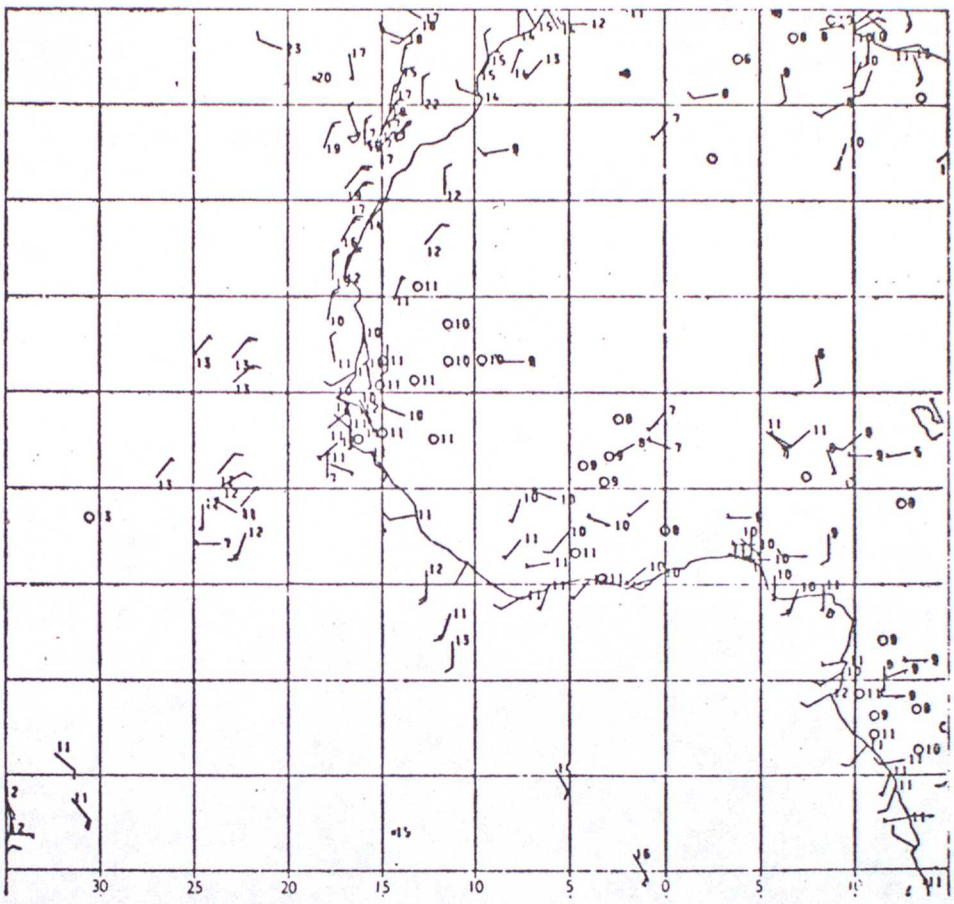

Figure 6a Data for 1000 mb. 12Z 2 September 1974. 1000 mb heights in metres: full fleche = 5 m sec^{-1}.

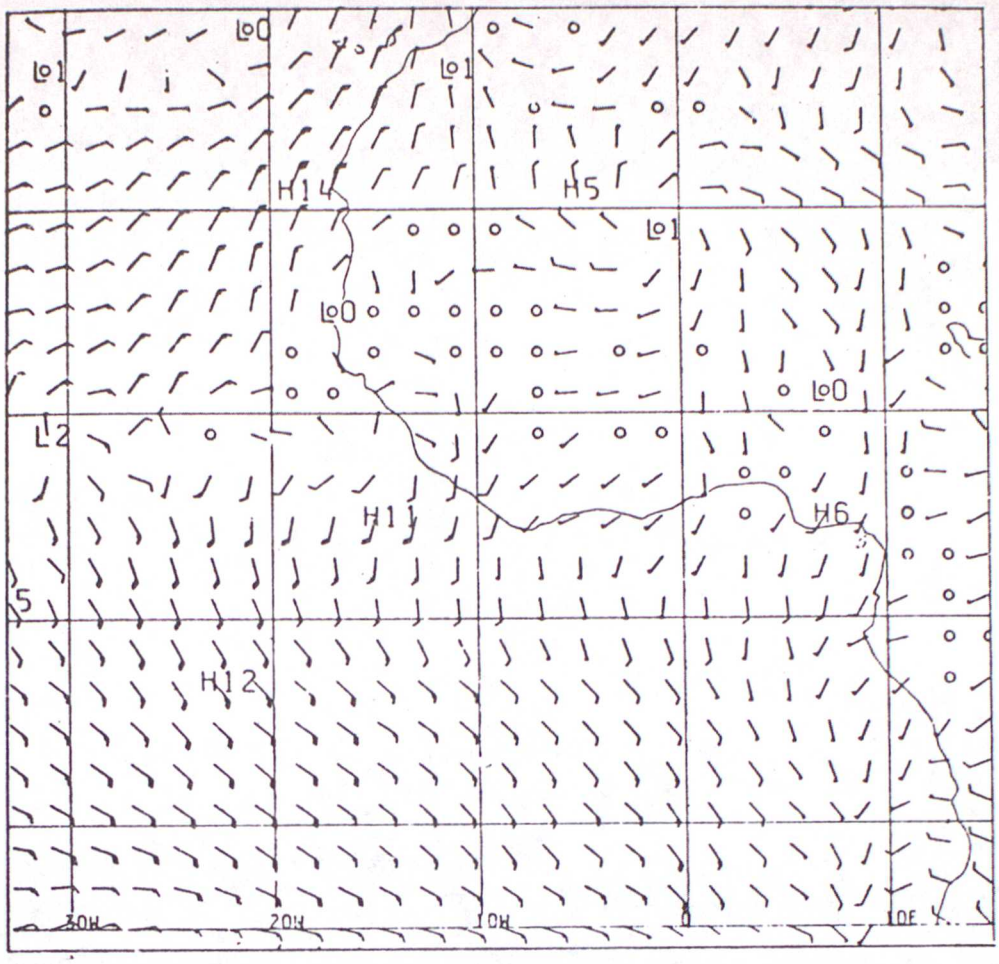

Figure 6b Part of the objective analysis of the wind field. 1000 mb 12Z 2 September 1974. Full fleche = 5 m sec^{-1}.

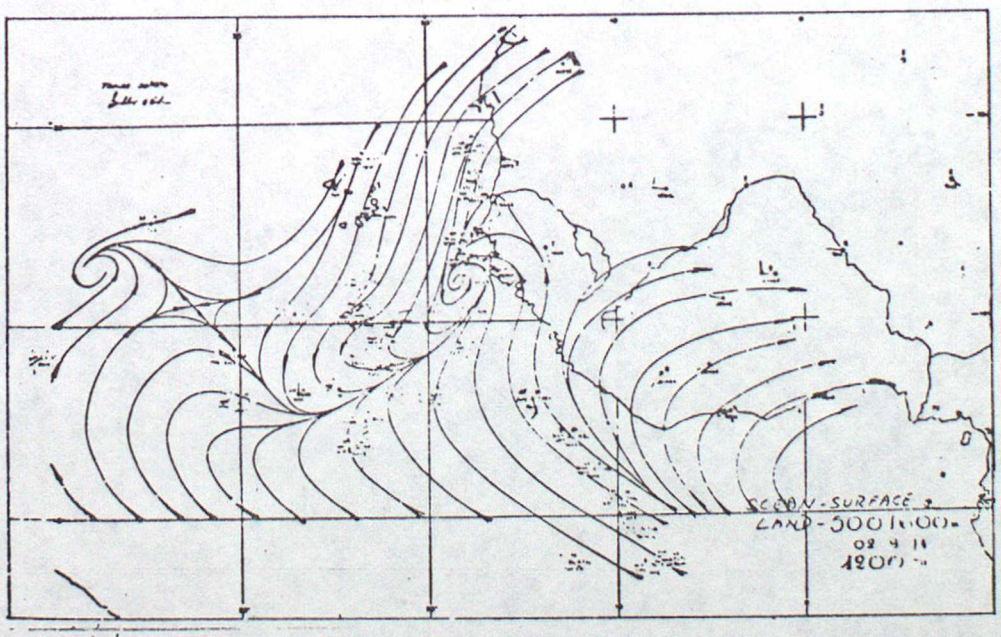

Figure 6c Subjectively analysed stream function 12Z 2 September 1974. Surface wind over ocean; 500/600 m wind over land.

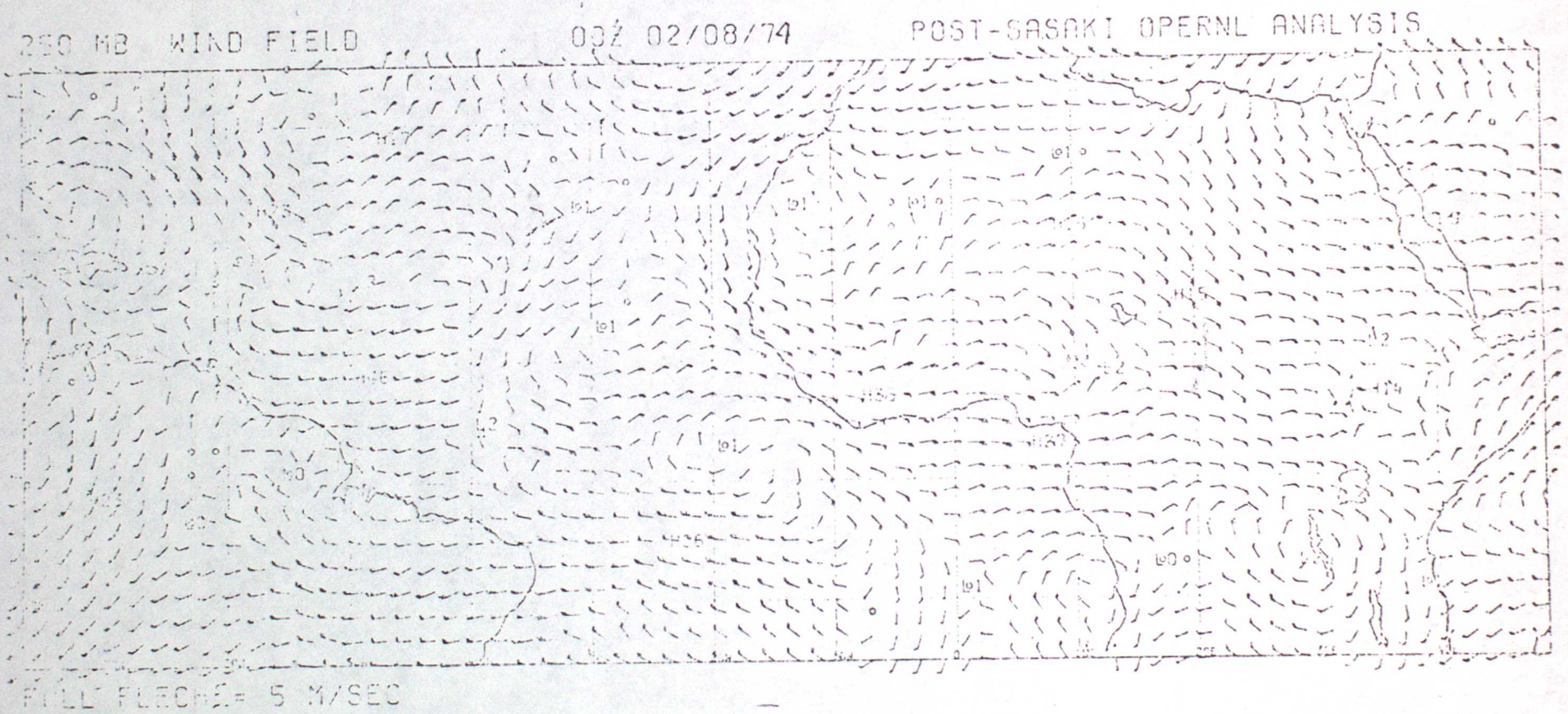

Figure 7a Objective analysis of winds at 250 mb for 00Z 2 August 1974.

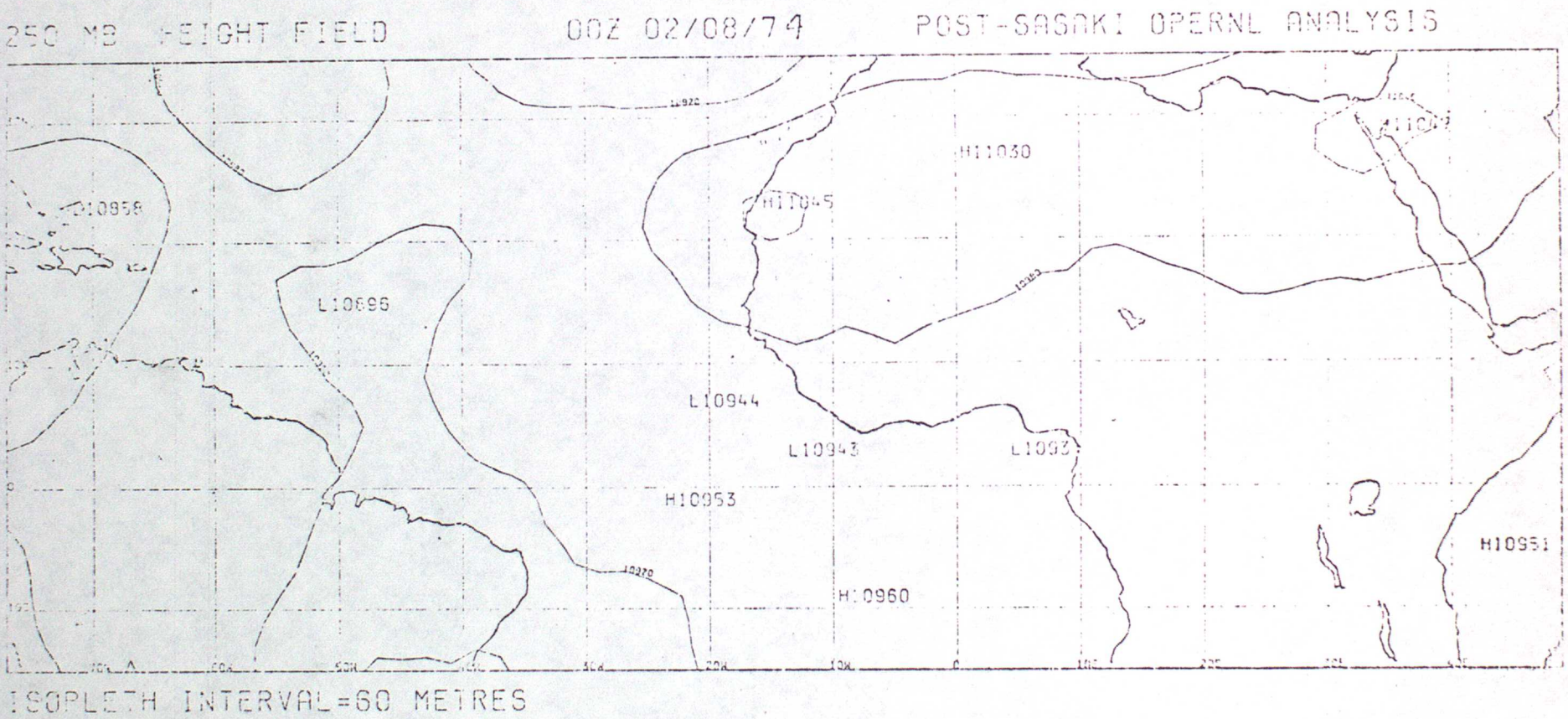

Figure 7b Objective analysis of heights at 250 mb for 00Z 2 August 1974

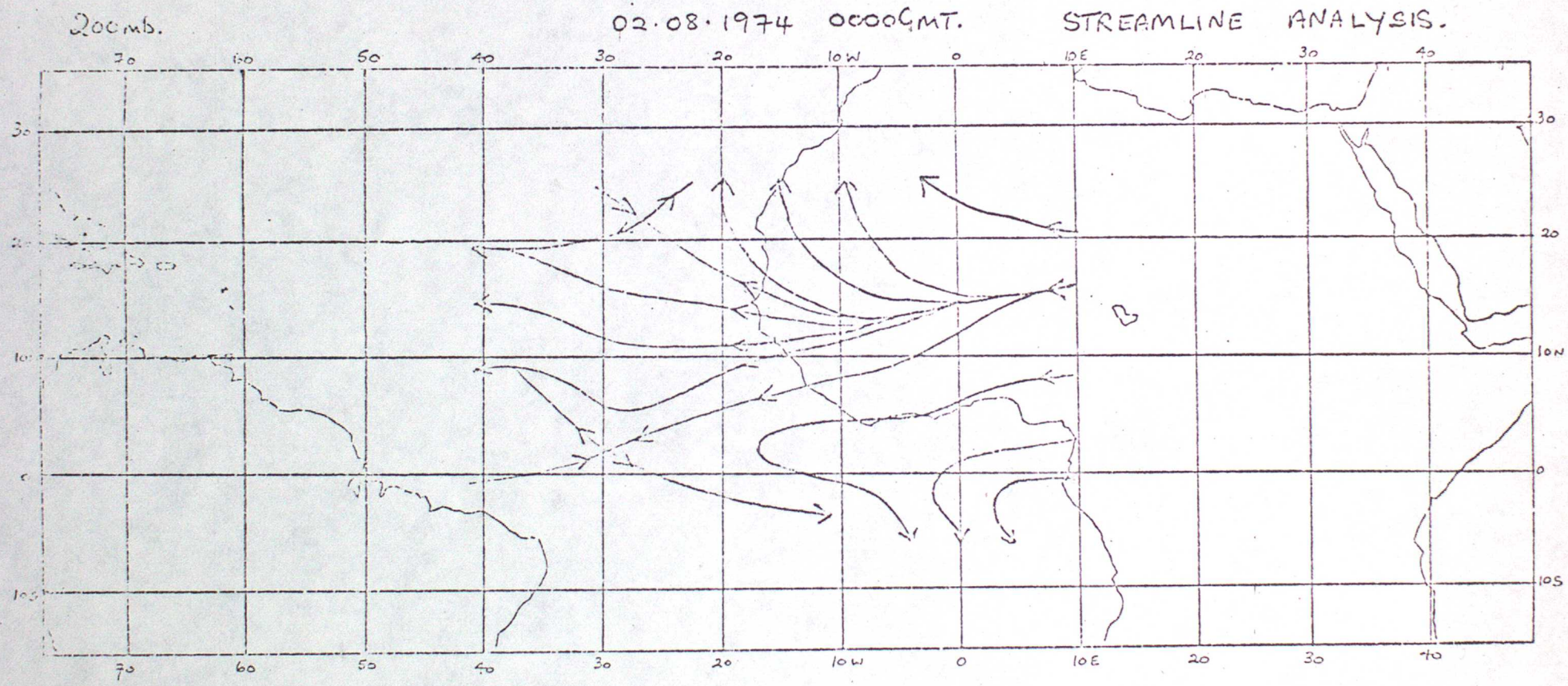

Figure 7c Hand-drawn 200 mb streamline analysis for 00Z 2 August 1974.

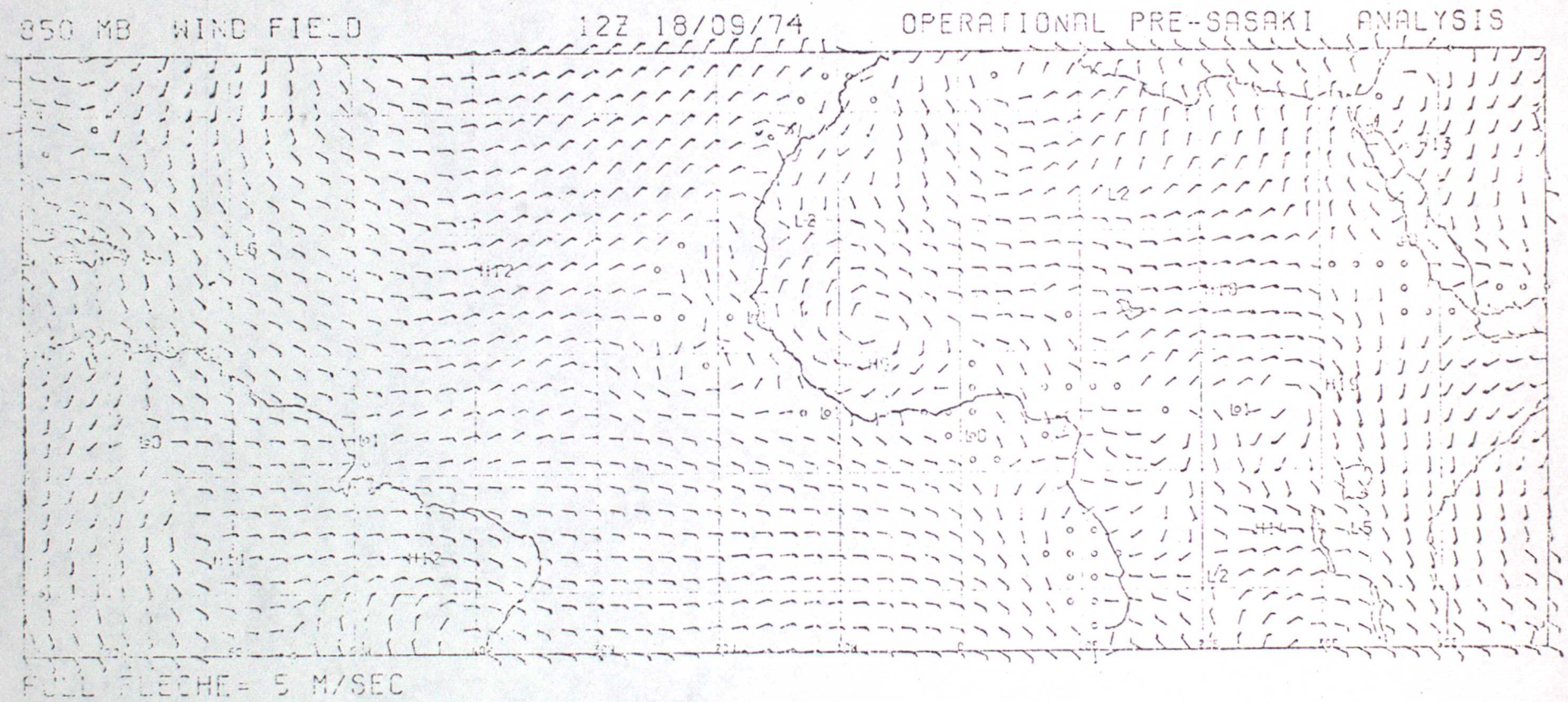

Figure 8a Objective analysis of winds at 850 mb for 12Z 18 September 1974 before the Sasaki variational step.

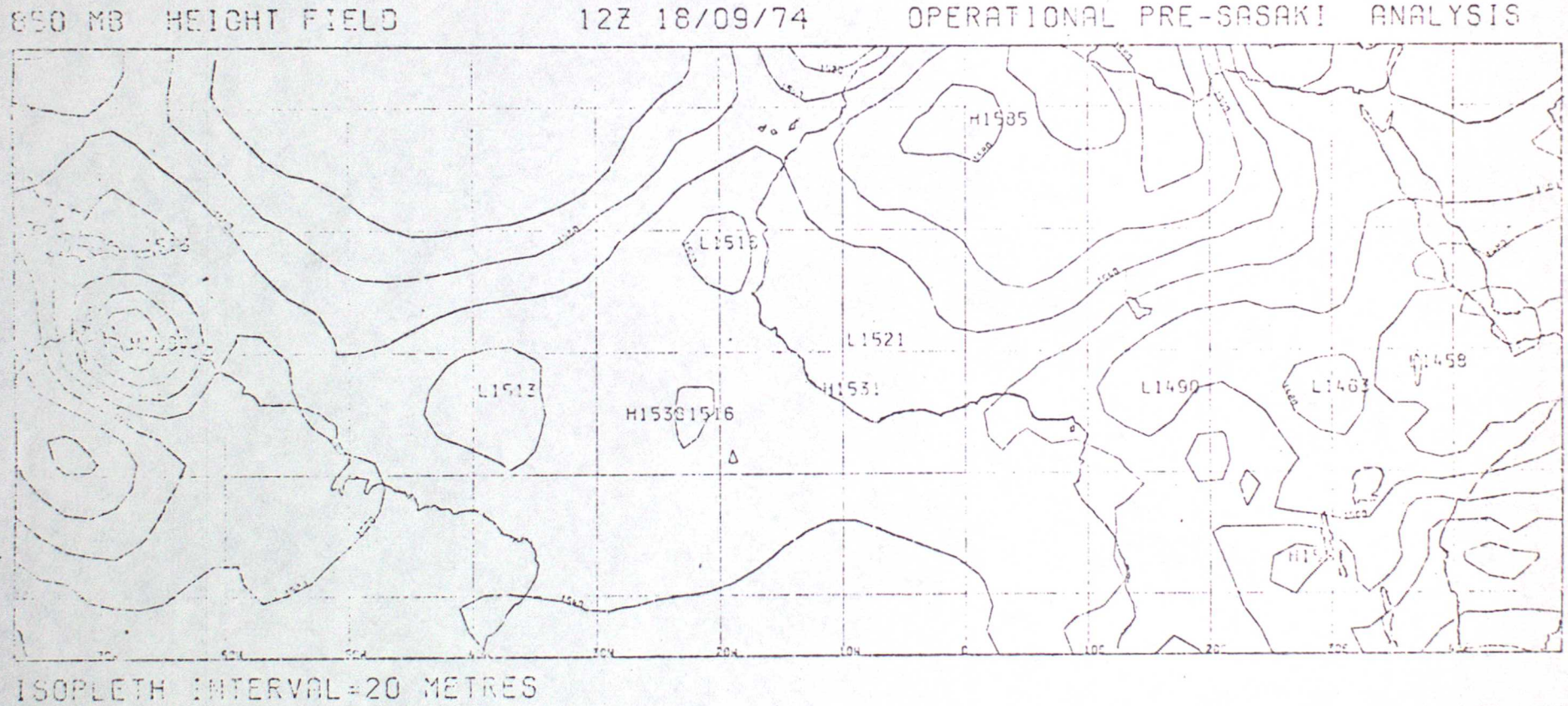

Figure 8b Objective analysis of heights at 850 mb for 12Z 18 September 1974 before the variational step.

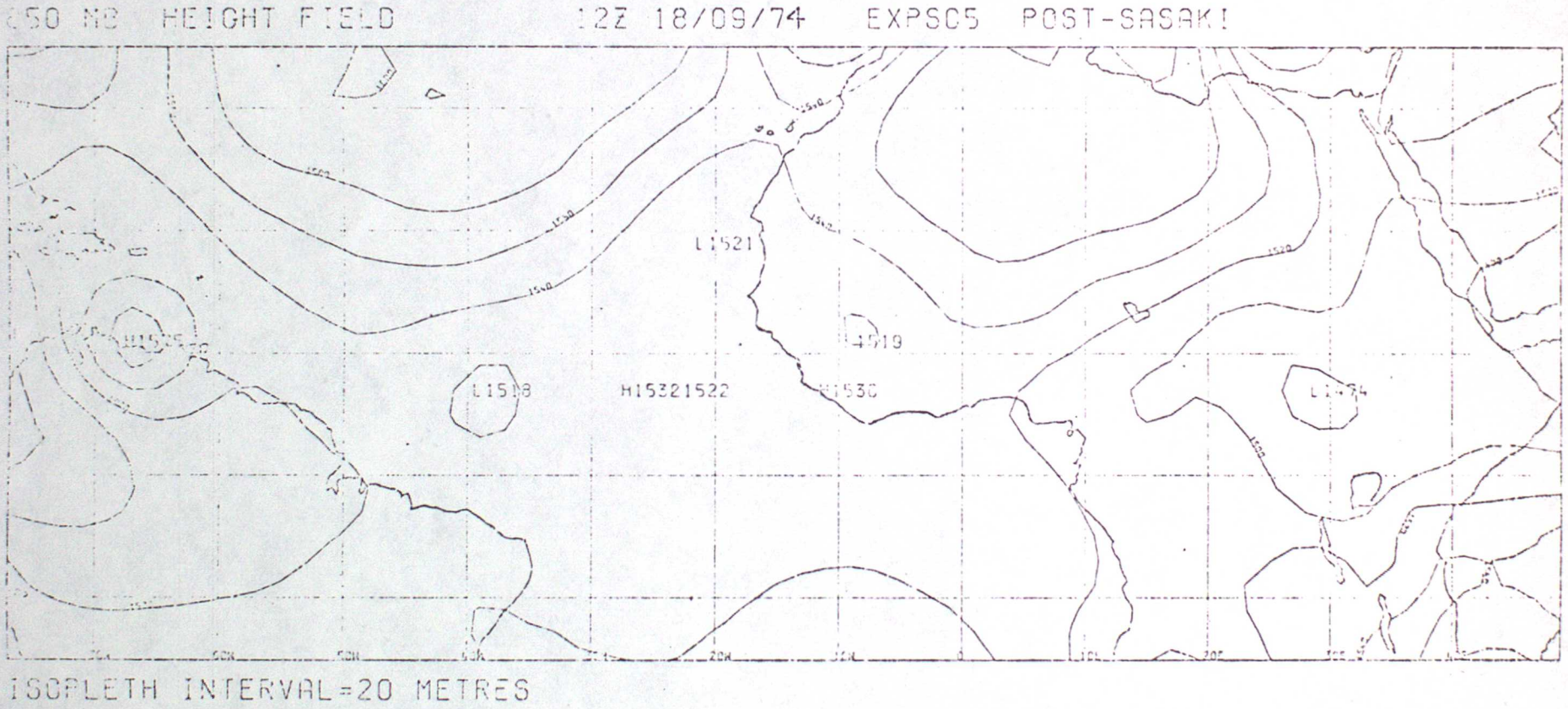

Figure 8c Objective analysis of heights at 850 mb for 12Z 18 September 1974 following the variational step.

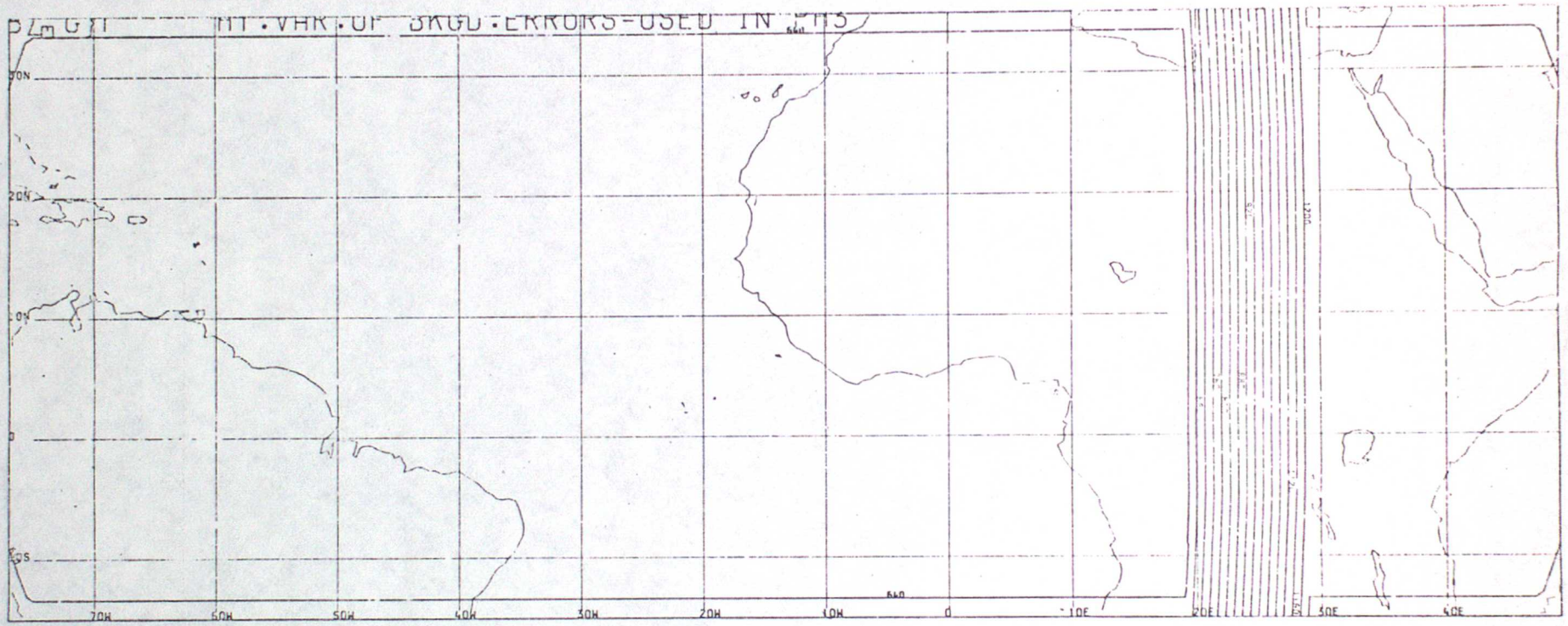

Figure 9a Values of the variance of the background field errors (heights) used during Phase III of GATE

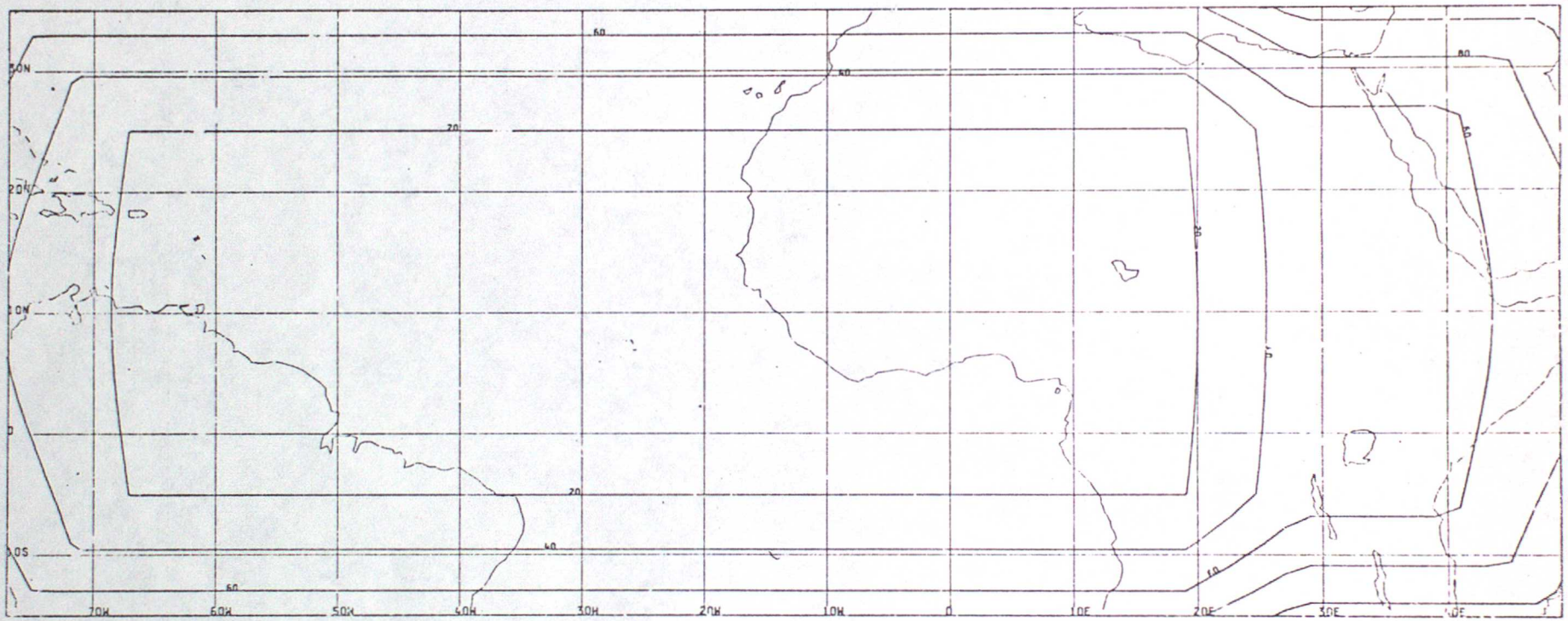

ISOPLETH INTERVAL=20 METRES^2 SEC^{-2}

Figure 9b Values of the variance of the background field errors (winds) used during Phase III of GATE

APPENDIX 1. PRELIMINARY ESTIMATES OF THE VARIANCE OF ERRORS OF THE BACKGROUND FIELD

As noted in § 4 no relevant statistics were available to provide estimates of the errors of the background field prior to the GATE tests. The following approach was used, however, to make some estimates as to what these might be and though, in the event, these values turned out to be considerably over optimistic, as discussed in § 4, we include an account of the preliminary derivation here for completeness. We consider the primary background fields first. Reference to § 3 indicates that there are several components of error in those fields, namely:

a. Persistence around the boundary.

b. Pure forecast away from the boundary.

c. A small percentage of climatology.

However, since only 1% of climatology is added into the background field, the contribution to the error from this component can essentially be neglected.

Let us first consider the persistence component. If we denote the autocorrelation of a meteorological variable over a time Δt by $R(\Delta t)$ then, assuming the climatological standard deviation σ_c^2 to be known, the standard deviation of persistence errors appropriate to Δt, σ_p^2 is given by:

$$\sigma_p^2 = 2\sigma_c^2 (1 - R(\Delta t)) \qquad \text{(A1)}$$

To derive the forecast component we make the assumption that, away from the boundary, the variance of forecast errors ($\overline{\Delta^2}$) would be proportional to the variance of the persistence errors

i.e. $$\overline{\Delta^2} = K^2 \sigma_p^2$$

or $$\overline{\Delta^2} = 2K^2 \sigma_c^2 (1 - R(\Delta t)) \qquad \text{(A2)}$$

This expression is valid for the errors of the primary background fields. To obtain appropriate values for the secondary levels, the modification to the background field following the analysis of primary levels (§3) should additionally have been taken into account. However, in view of the uncertainties involved in the estimates this was not done and the above expression was applied to these fields also, with values consistent with those for the primary levels.

For the operation of the analysis scheme during GATE, the 12 hour correlation between winds or heights in the tropics was taken to be about 0.7 (Jenkinson; personal communication); K, by direct comparison with values derived from 10 level model monthly rms errors, took the values displayed in Table A1.1. The boundary values, given by equation (A1) were approached by allowing K to vary linearly from its internal value to unity over a number of grid lengths.

Consultation of available literature (e.g. Tucker, 1960) showed that σ_c^2 could be adequately expressed for each level as a function of latitude, ϕ, in the form

$$\sigma_c^2 = a(p) + b(p)(\phi - 10^\circ)^2$$

where a(p) and b(p) took the values shown in Table A1.2 for heights and winds.

p mb	K (heights)	K (winds)
1000	1.0	1.0
950	1.0	1.0
850	0.8	0.7
700	0.7	0.5
500	0.7	0.6
400	0.7	0.6
300	0.7	0.5
250	0.7	0.5
200	0.7	0.5
150	0.7	0.5
100	0.8	0.7
70	0.8	0.7
30	1.0	1.0
10	-	-

Table A1.1 Values of K (equation (A2)) used during the operation of the analysis scheme throughout GATE, appropriate to height and wind analyses respectively.

Pressure	Heights		Winds	
	a(p)	b(p)	a(p)	b(p)
1000	13.0	.0224	13.26	.0102
950	13.0	.0224	13.26	.0102
850	15.0	.0080	7.43	.0249
700	17.0	.0128	15.91	.0249
500	20.0	.032	17.50	.0486
400	30.0	.032	21.75	.0761
300	45.0	.032	25.99	.1036
250	55.0	.032	50.39	.0948
200	55.0	.040	50.39	.0948
150	50.0	.048	40.58	.0745
100	50.0	.032	38.32	.0458
70	60.0	0.0	29.84	.0146

Table A1.2. Climatological Variability Constants

APPENDIX 2. CRITERION FOR DATA CHECKING

Let $\bar{s}$ be the value of our estimate at the observation point derived from the surrounding observations. This will be normally distributed with mean the truth $\hat{s}$ and variance $\overline{E^2}$ (which we can determine). s_o (observed value) will be normally distributed with mean $\hat{s}$ and variance $\overline{\epsilon_o^2}$ if the observation is to be considered acceptable for analysis. If the observation is to be considered unacceptable then we will assume that s_o will still be normally distributed with mean $\hat{s}$, but the variance will be $\overline{\epsilon_w^2} \gg \overline{\epsilon_o^2}$. Therefore the problem of resolving whether an observation is acceptable or unacceptable can be reduced to determining whether $(\bar{s} - s_o)$ is a member of a population which is normally distributed with mean zero and variance $\overline{E^2} + \overline{\epsilon_o^2}$ or a member of a similar population with variance $\overline{\epsilon_w^2} + \overline{E^2}$. Writing y for the value of $(\bar{s} - s_o)$ the test which we require is as follows:

We reject the hypothesis that the observation is acceptable if

$$\frac{Pr\{(\bar{s} - s_o) = y \text{, given observation acceptable}\}}{Pr\{(\bar{s} - s_o) = y \text{, given observation unacceptable}\}} < c$$

i.e.

$$\frac{\exp\left(-\frac{y^2}{2(\overline{E^2} + \overline{\epsilon_o^2})}\right)}{\exp\left(-\frac{y^2}{2(\overline{\epsilon_w^2} + \overline{E^2})}\right)} < c'$$

Therefore

$$\exp\left\{+\frac{y^2}{2}\left[\frac{1}{\overline{\epsilon_w^2} + \overline{E^2}} - \frac{1}{\overline{E^2} + \overline{\epsilon_o^2}}\right]\right\} < c'$$

$$\exp\left\{-\frac{y^2}{2}\left[\frac{\overline{\epsilon_w^2} - \overline{\epsilon_o^2}}{(\overline{\epsilon_w^2} + \overline{E^2})(\overline{E^2} + \overline{\epsilon_o^2})}\right]\right\} > \frac{1}{c'}$$

i.e.

$$\frac{y^2}{2} > \log\left(\frac{1}{c'}\right) \cdot (\overline{E^2} + \overline{\epsilon_o^2}) \left\{\frac{\overline{\epsilon_w^2} + \overline{E^2}}{\overline{\epsilon_w^2} - \overline{\epsilon_o^2}}\right\}$$

i.e.

$$|y| > \sqrt{2 \log \frac{1}{c'}} \sqrt{\overline{\epsilon_o^2} + \overline{E^2}} \sqrt{\frac{\overline{\epsilon_w^2} + \overline{E^2}}{\overline{\epsilon_w^2} - \overline{\epsilon_o^2}}}$$

If we assume that $\overline{\epsilon_w^2} \gg \overline{E^2}$; $\overline{\epsilon_w^2} \gg \overline{\epsilon_o^2}$ then our test reduces to rejecting the hypothesis that an observation is correct if

$$|\bar{s} - s_o| > \sqrt{2 \log \frac{1}{c'}} \sqrt{\overline{\epsilon_o^2} + \overline{E^2}}$$

where c' may be suitably determined from the power of the test which we require.

APPENDIX 3. A METHOD FOR THE TREATMENT OF GRID SCALE AND SUB GRID SCALE FEATURES

The scale of features that can be represented in an objective analysis depends on both the grid length, a, and the spacing of the observations. In particular features of scale less than two or three grid lengths cannot be represented on the grid so that we are, in effect, analysing scales of motion only down to this limit. The observations will obviously be influenced by phenomena on all scales however, the smaller scale features affecting their representivity for analysis of larger scales, and the possibility arises that features of wavelength, say, 2a may actually be interpreted by the analysis scheme as being of wavelength 2a or more. This may particularly occur if two or more observations are close enough to be similarly influenced by such a small scale feature. The generation of such spurious waves in the analysis is obviously undesirable and such effects should be excluded as far as possible, whilst, at the same time, taking account of the influence of the small scale features on the observations. We begin by separating the spectrum of waves into a number of wavebands:

M - medium and long waves which we wish to analyse.

S - short waves, too short to analyse, but long enough for the correlation function to be significant over a grid length.

N - noise of such small linear dimension that it can be regarded as uncorrelated in space.

Then, if the observations are affected by all scales of motion we may write

$$s_i = \hat{s}_i + \epsilon_{oi} = \hat{s}_{Mi} + \hat{s}_{Si} + \hat{s}_{Ni} + \epsilon_{oi}$$

However, if the background field can be assumed to have had the short wave features filtered out (§ 3) we have

$$\tilde{s}_i = \tilde{s}_{Mi} \quad \text{only}$$

Now, since the aspect of the 'truth' we are trying to analyse is $\hat{s}_{Mg}$, then, going through the analysis as before, defining quantities

$$\Delta_{Mi} = \hat{s}_{Mi} - \tilde{s}_{Mi} \qquad \Delta_{Mg} = \hat{s}_{Mg} - \tilde{s}_{Mg}$$

and making the assumption that covariances between waves on different scales are zero, we find the coefficients of the matrix $\underline{\underline{A}}$ corresponding to equation (5) to be

$$A_{ij} = \overline{\Delta_{Mi}\Delta_{Mj}} + \overline{\Delta_{Mg}\Delta_{Mg}} - \overline{\Delta_{Mi}\Delta_{Mg}} - \overline{\Delta_{Mj}\Delta_{Mg}} + \overline{\hat{s}_{Si}\hat{s}_{Sj}} \qquad i \neq j;\ i,j \neq n+1$$

$$A_{ii} = \overline{\Delta_{Mi}\Delta_{Mi}} - 2\overline{\Delta_{Mi}\Delta_{Mg}} + \overline{\Delta_{Mg}\Delta_{Mg}} + \overline{\epsilon_{oi}^2} + \overline{\hat{s}_{Ni}\hat{s}_{Ni}} + \overline{\hat{s}_{Si}\hat{s}_{Si}} \qquad i \neq n+1$$

$$A_{i,n+1} = \overline{\Delta_{Mg}\Delta_{Mg}} - \overline{\Delta_{Mi}\Delta_{Mg}} \qquad i \neq n+1$$

$$A_{n+1,n+1} = \overline{\Delta_{Mg}\Delta_{Mg}} .$$

We see that most of the terms of equation (5a) are the same as for equation (5) with Δ_M instead of Δ, but with additional terms in A_{ij} and A_{ii} involving the short wave and noise components only. Note that these additional terms express correlations only between observations, since short waves and noise are not present in the background field. The noise term occurs only where ϵ_{oi}^2 occurs and therefore has the same effect as that of the observational errors; the terms $\hat{s}_{Si}\hat{s}_{Sj}$ $(i \neq j)$ will only arise if observations are close enough to

one another, otherwise (when i = j) the short wave terms again have the same effect as observational errors.

It is evident that if we are to carry out the analyses making full allowance for noise etc., we need to have values of $\overline{\Delta_{Mi}\Delta_{Mj}}$, $\overline{\hat{S}_{Si}\hat{S}_{Sj}}$, $\overline{\hat{S}_{Ni}\hat{S}_{Ni}}$ etc.

These values are, in principle, determinable by a method discussed by Rutherford (1972) whereby correlation functions are calculated from observations and model forecasts, the empirical curves transformed into spectral space, the spectral range divided into bands S, M and N and the correlation curves obtained for these wavebands. At the time of GATE, however, no such detailed statistics for the model error were available so that the simple approach described in § 4 was adopted.

APPENDIX 4. SPECIFICATION OF THE VARIANCE OF ERRORS OF OBSERVATION

A4.1 HEIGHT OBSERVATIONS

a. Surface height observations. These were held constant and specified as follows:

1000 mb land	$\overline{\epsilon_o^2}$	$= 44\ m^2$
950 mb land	$\overline{\epsilon_o^2}$	$= 44\ m^2$
850 mb land	$\overline{\epsilon_o^2}$	$= 44\ m^2$
1000 mb ships	$\overline{\epsilon_o^2}$	$= 44\ m^2$

i.e. one value for all observations.

b. Upper air land observations. Values of $\overline{\epsilon_{70}^2}$ were available for each station. Values of $\overline{\epsilon^2}$ at lower levels were obtained from the equation

$$\overline{\epsilon_p^2} = \overline{\epsilon_{70}^2} \left[\frac{\log(p/1000)}{\log(70/1000)} \right]^2$$

This assumes a constant temperature error throughout the ascent. A lower limit of 44 m^2 was chosen for the value of $\overline{\epsilon_p^2}$ at any level, however, equivalent to the error in a 1000 mb surface observation.

Different values of $\overline{\epsilon_{70}^2}$ were chosen depending on whether, in fact, the ascents were adjusted with the random error correction described in § 2. If an ascent had been corrected, the value of ϵ_{70}^2 was amended to a new value σ_{70}^2 given by the formula

$$\overline{\sigma_{70}^2} = \overline{\epsilon_{70}^2} \left[0.64 + 4 \times 10^{-6} A^2 \right]$$

where A is the observed error at 70 mb (assuming the analysed field to be the "truth"). This equation may be deduced as follows.

Let $\overline{\epsilon_{70}^2}(\min)$, $\overline{\sigma_{70}^2}(\min)$ be minimum values of $\overline{\epsilon_{70}^2}$ and $\overline{\sigma_{70}^2}$ for all types of sonde. When A = 0, a reasonable estimate for σ_{70}^2 is given by

$$\overline{\sigma_{70}^2} = \frac{\overline{\sigma_{70}^2}(\min)}{\overline{\epsilon_{70}^2}(\min)} \overline{\epsilon_{70}^2} = k \overline{\epsilon_{70}^2}$$

As A grows larger, we should want the value of $\overline{\sigma_{70}^2}$ to grow larger, as our estimate of the correction is less reliable. We therefore take

$$\overline{\sigma_{70}^2}(A) = k \overline{\epsilon_{70}^2} + A^2 \alpha$$

We now make the assumption that at the value of A for rejection the value of $\sigma_{70}^2(A)$ has reached the value for uncorrected sondes of that type. Therefore at A = 300 m

$$\overline{\sigma_{70}^2}(300) = k \overline{\epsilon_{70}^2} + 300^2 \alpha = \overline{\epsilon_{70}^2} \quad \text{so} \quad \alpha = \frac{\overline{\epsilon_{70}^2}}{300^2}(1-k)$$

From evidence available, a minimum value of $\overline{\epsilon_{70}^2}$ of $(25\ m)^2$ and of $\overline{\sigma_{70}^2}$ of $(20\ m)^2$ appears realistic. k therefore takes the value 0.64 and so α becomes $4 \times 10^{-6}\ \overline{\epsilon_{70}^2}$ and the formula follows.

c. Upper air ship observations. The errors were specified as for upper air land observations. Initially, however, no values of $\overline{\epsilon_{70}^2}$ were available for individual ships. $\overline{\epsilon_{70}^2}$ was therefore set to a constant value ($900\ m^2$) for all ships.

d. SIRS observations. The error for SIRS was initially specified to be of the form

$$\epsilon^2(p) = \epsilon_o^2(p) + [K(p)\,\Delta t]^2$$

where the error of the observation is given by

$$\epsilon_o^2(p) = [172 - 44 \log_{10} p]^2$$

and allowance for the time lag by $[K(p)\,\Delta t]^2$ where, with ϕ = latitude in degrees,

$$K(\phi, p) = a(p) + b(p)(\phi - 10°)^2$$

During GATE, however, both a(p) and b(p) were set to zero so that no allowance for time lag was made.

A4.2 Wind observations

a. Surface wind observations. 850 mb land wind observations were not used. Other observations were used, however, and errors specified as follows.

1000 mb land	$\overline{\epsilon_o^2} = 1\ m^2\ sec^{-2}$	
950 mb land	$\overline{\epsilon_o^2} = 1\ m^2\ sec^{-2}$	(not used since 950 mb winds not analysed).
1000 mb ship	$\overline{\epsilon_o^2} = 4\ m^2\ sec^{-2}$	

b. Upper air land observations. The error for pressure level, p, for RADAR and PILOT observations was set to

$$\overline{\epsilon_p^2} = [4.9 - 1.4 \log_{10} p]^2\ m^2\ sec^{-2}$$

c. Upper air ship observations. RADAR winds were treated as for b. above; OMEGA winds were allocated errors according to ship position by reference to a field of grid square values available (Figure A4.1). The same value of error was used at each level.

d. AIREPS Each observation was allocated to the analysis levels immediately above and below the observation level with correction to take into account the vertical wind shear (§ 2). The error of each component was specified as

$$\overline{\epsilon^2_{comp}} = \overline{\epsilon_o^2} + 2\sigma_c^2 (1 - R(12\ hours)) \frac{|\Delta t|}{12} + 0.06\,|dp|$$

which, with R (12 hours) = 0.7 (Appendix 1) reduces to

$$\overline{\epsilon^2_{comp}} = \overline{\epsilon_o^2} + 0.05\,\sigma_c^2 |\Delta t| + 0.06\,|dp|$$

where Δt is the time difference in hours between the analysis and observation times; σ_c^2 is the climatological variability (Appendix 1) and dp is the difference between the observation and analysis levels. The first term on the

RHS is the observation error, the second describes the error due to the time lag whilst the third term allows for the error of interpolation from observation to analysis levels. $\overline{\epsilon_o^2}$ was set to $(1.2 \text{ m sec}^{-1})^2$ for spot winds; $(3.6 \text{ m sec}^{-1})^2$ for mean winds.

e. GOES winds. By analogy with AIREPS the errors for these were set to

$$\overline{\epsilon^2_{comp}} = \overline{\epsilon_o^2} + 0.05\,\sigma_c^2\,|\Delta t|$$

$\overline{\epsilon_o^2}$ was set to $(5.4 \text{ m sec}^{-1})^2$ for the 850 mb level.

$(8.6 \text{ m sec}^{-1})^2$ for the 250 mb level.

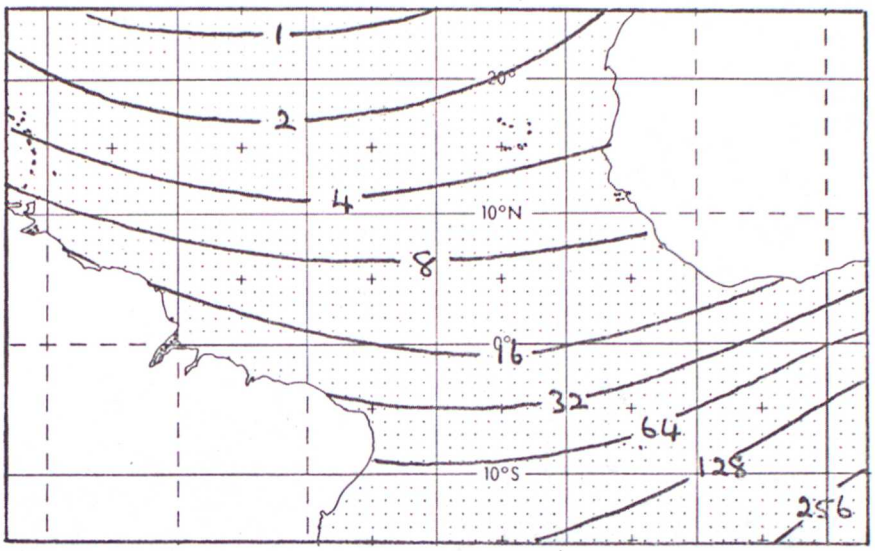

Figure A4.1 Errors of observation for omega winds used during GATE (m^2 sec^{-2})